Environmental Science & Technology

Article

Cite This: Environ. Sci. Technol. 2018, 52, 12829−12840

pubs.acs.org/est

Down-Regulation of *hspb9* and *hspb11* Contributes to Wavy Notochord in Zebrafish Embryos Following Exposure to Polychlorinated Diphenylsulfides

Rui Zhang,[†] Xiaoxiang Wang,[§,∥] Xuesheng Zhang,[⊥] Junjiang Zhang,[§] Xiaowei Zhang,[§] Xiao Shi,[#] Doug Crump,[▽] Robert J. Letcher,[▽] John P. Giesy,[○] and Chunsheng Liu*[,‡]

[†]School of Resources and Environment, University of Jinan, Jinan 250022, P. R. China

[‡]College of Fisheries, Huazhong Agricultural University, Wuhan 430070, P. R. China

[§]State Key Laboratory of Pollution Control and Resources Reuse, School of the Environment, Nanjing University, Nanjing 210023, P. R. China

[∥]Association of Chinese Chemists and Chemical Engineers in Germany, Limburgerhof 67117, Germany

[⊥]School of Resources and Environmental Engineering, Anhui University, Hefei 230601, P. R. China

[#]Center for Reproductive Medicine, Department of Obstetrics and Gynaecology, Nanfang Hospital, Southern Medical University, Guangzhou 510515, P. R. China

[▽]Ecotoxicology and Wildlife Health Division, Environment and Climate Change Canada, National Wildlife Research Centre, Carleton University, 1125 Colonel By Drive, Ottawa, K1A 0H3, Canada

[○]Department of Veterinary Biomedical Sciences and Toxicology Centre, University of Saskatchewan, Saskatoon, Saskatchewan S7N 5B3, Canada

Supporting Information

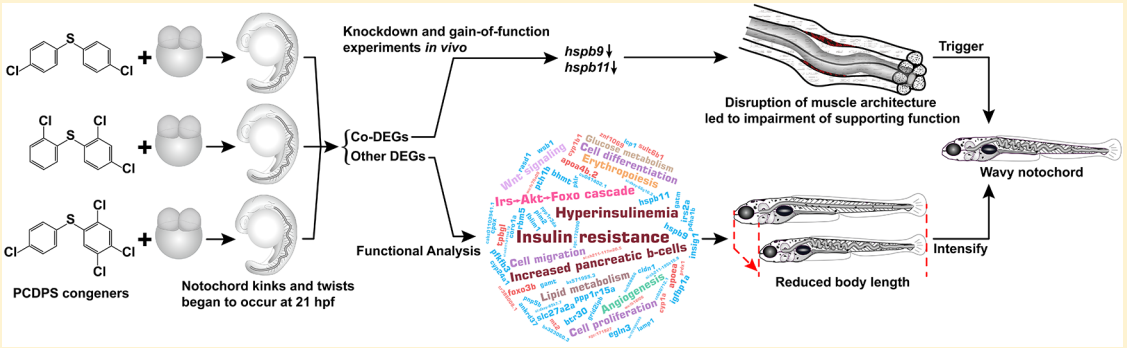

ABSTRACT: It is hypothesized that key genes, other than *ahr2*, are present and associated with the development of a unique type of notochord malformation known as wavy notochord in early life stages of zebrafish following exposure to polychlorinated diphenylsulfides (PCDPSs). To investigate the potential mechanism(s), time-dependent developmental morphologies of zebrafish embryos following exposure to 2500 nM 2,4,4′,5-tetra-CDPS, 2,2′,4-tri-CDPS or 4,4′-di-CDPS were observed to determine the developmental time point when notochord twists began to occur (i.e., 21 h-postfertilization (hpf)). Simultaneously, morphometric measurements suggested that PCDPS exposure did not affect notochord growth at 21 or 120 hpf; however, elongation of the body axis was significantly inhibited at 120 hpf. Transcriptome analysis revealed that the retardation of body growth was potentially related with dysregulation of transcripts predominantly associated with the insulin-associated Irs−Akt−FoxO cascade. Moreover, knockdown and gain-of-function experiments in vivo on codifferentially expressed genes demonstrated that reduced expression of *hspb9* and *hspb11* contributed to the occurrence of wavy notochord. The results of this study strongly support the hypothesis that the notochord kinks and twists are triggered by the down-regulation of *hspb9* and *hspb11*, and intensified by body growth retardation along with normal notochord length in PCDPS-exposed zebrafish embryos.

INTRODUCTION

Polychlorinated diphenylsulfides (PCDPSs) (Figure 1A) are a group of halogenated aromatic compounds comprised of 209 theoretically possible congeners with structural similarities to

Received: August 11, 2018
Revised: October 16, 2018
Accepted: October 18, 2018
Published: October 18, 2018

DOI: 10.1021/acs.est.8b04487
Environ. Sci. Technol. 2018, 52, 12829−12840

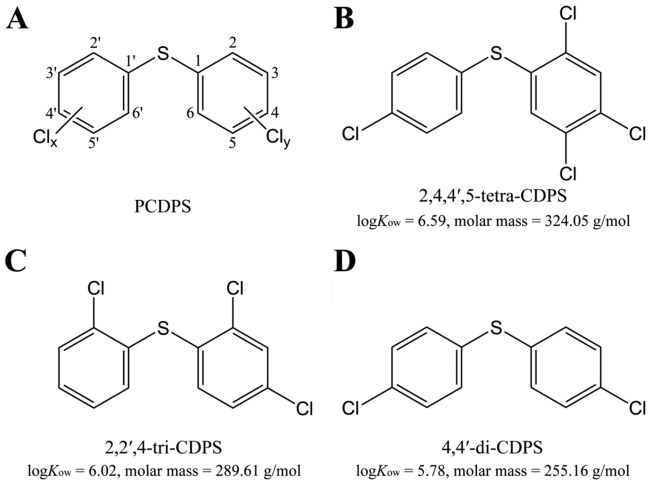

Figure 1. Generalized structure of polychlorinated diphenylsulfides (PCDPSs) (A) and structural formulas, log*K*ow values, and molar masses of the three congeners tested in this study: 2,4,4′,5-tetra-CDPS (B), 2,2′,4-tri-CDPS (C) and 4,4′-di-CDPS (D).

polychlorinated diphenyl ethers (PCDEs), polychlorinated biphenyls (PCBs) and polybrominated diphenyl ethers (PBDEs). They have been widely used as lubricants,[1] flame retardants,[2] insulating media,[2] and acaricides[3−7] in many countries like China and the U.S. To date, PCDPSs have been frequently found in a variety of environmental matrices, including industrial wastewater and dust,[8,9] waste incineration ash,[8] natural waters,[10,11] and even crops like fruits[7] and tea leaves,[4] ranging from monochloro- to heptachloro-diphenyl sulfide congeners. However, due to the lack of pure authentic standards for PCDPS and/or the shortcomings of purification and analytical methods, most previous studies on concentrations of PCDPSs in environmental matrices were based on qualitative reporting. Only one recent study quantitatively examined total concentrations of 19 PCDPS congeners in surface water and sediment from the Nanjing section of the Yangtze River; concentrations ranged from 0.18 to 2.03 ng/L and 0.10 to 6.90 ng/g dry weight, respectively.[11]

A growing number of studies have suggested that PCDPSs could cause a spectrum of adverse effects, such as hepatic oxidative stress,[12−14] retardation of development,[15] reproductive disorders,[15] and even increased mortality[13,15−17] in vertebrates like mammals, fish and birds. Increased mortality was recently shown to be initiated and mediated by activation of the aryl hydrocarbon receptor 2 (Ahr2).[17] Several PCDPS congeners have also been shown to activate the AHR and subsequently modulate expression of genes in vitro in mammals and birds.[18,19] Furthermore, given the physicochemical characteristics similar to other persistent organic pollutants (POPs), including environmental persistence,[20] long-range transport potential,[20] and bioaccumulation potential,[17,21,22] PCDPSs have been regarded as a group of potential dioxin-like compounds (DLCs) of high priority concern.

In a previous study, acute exposure to dichloro- to heptachloro-diphenyl sulfide congeners in early life stages of zebrafish resulted in significant teratogenic effects, such as spinal curvature, malformations of the tail, yolk sac edema, and pericardial edema.[17] These malformations were generally classified as classical, dioxin-like effects. However, a unique type of notochord malformation, namely a strikingly wavy notochord, was noted in zebrafish larvae exposed to PCDPS.[17] Exposure of zebrafish to 1.55 nM 2,3,7,8-tetrachlorodibenzo-*p*-dioxin (TCDD) resulted in spinal curvatures,[23,24] but the kinking/bending of the notochord was much more severe in PCDPS-exposed zebrafish at generally similar TCDD-equivalent concentrations.[17] Thus, it is hypothesized that molecular mechanism(s) underlying the notochord malformations extend beyond Ahr2 activation and perhaps occur downstream of Ahr2 or other nuclear receptors/transcription factors in zebrafish embryos exposed to PCDPS. It has been suggested that AHR-mediated developmental toxicity of xenobiotics involves dysregulation of as-yet unidentified transcriptional intermediates.[25] In addition, down-regulation of *sox9b* gene was associated with jaw malformations in TCDD-exposed zebrafish embryos.[26] These findings support the hypothesis that additional molecular mechanisms are involved in malformations of the notochord of zebrafish exposed to PCDPSs.

In acute exposures to six individual PCDPS congeners (dichloro- to heptachloro-diphenylsulfides), the wavy notochords were most prevalent in zebrafish larvae exposed to 2500 nM 2,4,4′,5-tetra-CDPS, 2,2′,4-tri-CDPS and 4,4′-di-CDPS.[17] Individuals with wavy notochord accounted for almost all of the deformed larvae. Thus, to investigate mechanism(s) underlying PCDPS-induced wavy notochord, first, a time-dependent developmental morphology of zebrafish embryos/larvae was photographed and recorded following exposure to 2500 nM of each of the individual PCDPS congeners. The goal was to determine the defined developmental time point when the notochord twists began to occur. Second, a new batch of embryos was exposed in the same way and collected after specific durations of development for transcriptome analysis using RNA-seq to identify potential key codifferentially expressed genes (DEGs). Finally, knockdown and gain-of-function experiments in vivo were employed to determine which gene expression changes were associated with wavy notochord in developing zebrafish embryos. A potential molecular mechanism underlying PCDPS-induced wavy notochord in early life stages of zebrafish was identified and provided insights into pathways related to teratogenicity of dioxins/DLCs in early life stages of vertebrates.

MATERIALS AND METHODS

Chemicals and Reagents. The three PCDPS congeners under study—4,4′-di-CDPS, 2,2′,4-tri-CDPS, and 2,4,4′,5-tetra-CDPS (Figure 1B−D)—were synthesized previously by a palladium-catalyzed carbon−sulfur bond formation method.[27] The purities were determined to be >99% with no detectable dioxin-like polychlorinated dibenzo-*p*-dioxins and dibenzofurans (PCDDs/Fs) present as described previously.[19] All stock solutions of PCDPS congeners were prepared in dimethyl sulfoxide (DMSO, CAS number 67−68−5; >99.7% purity; Sigma-Aldrich, St. Louis, MO) and stored at −20 °C.

Animals and Waterborne Exposure Experiments. All husbandry and experimental procedures in the present study were approved by the Institutional Animal Care and Use Committee of the Huazhong Agricultural University and adhered to the Canadian Council on Animal Care guidelines for humane animal use. Adult wild-type zebrafish (AB strain, 7-month old) were maintained as described previously.[17] All fertilized eggs used in the present study were obtained by artificial fertilization to ensure the collected embryos were at the same developmental stage. Only those embryos undergoing normal development were selected for subsequent exposure

DOI: 10.1021/acs.est.8b04487
Environ. Sci. Technol. 2018, 52, 12829−12840

experiments by using a stereomicroscope (M205FA, Leica Microsystems, Wetzlar, Germany).

For in vivo waterborne exposures, the dosing solutions of PCDPS congeners were prepared immediately before use in embryonic rearing water (60 mg/L instant ocean salt in aerated distilled water) at a concentration of 2500 nM. The single concentration was selected based on results from a previous acute toxicity study.[17] The final concentration of DMSO in the exposure solutions was 0.5% (v/v).

Exposures were conducted in two parts. First, to determine the defined developmental time point when the twisted and kinked notochord was observed, the collected embryos were randomly distributed into glass beakers and exposed to each of the three individual PCDPS congeners or DMSO starting at 0.75 hpf. For each treatment, three replicate beakers were used, each containing 100 mL exposure solution and 100 embryos. Fifty percent of the exposure solution was renewed by freshly prepared exposure solution on a daily basis. Embryos were kept in an environmental chamber at controlled temperature (28 ± 0.5 °C) and photoperiod (12 h light and 12 h dark). During the 120-hpf exposure period (by which time, zebrafish have developed into free-swimming larvae and most organs have fully developed),[28] developmental morphology was observed every 2 h by use of a Leica M205FA stereomicroscope. Embryo/larva and notochord lengths of 20 individuals from each group were measured at 21 and 120 hpf using ImageJ software.[29] In the second part of the experiment, embryos were exposed to 2500 nM of each of the three PCDPSs or the solvent DMSO from 0.75 to 21 hpf. Three replicate beakers were included for each treatment containing 100 mL exposure solution and 100 embryos. At 21 hpf, 50 embryos from each replicate of the treatment and control groups were collected and immediately frozen in liquid nitrogen, and stored at −80 °C for RNA-seq Five other embryos from each treatment were sampled and fixed with 4% paraformaldehyde for subsequent confocal laser scanning microscopy of the notochord. The images were acquired as black and white micrographs using a Leica confocal microscope (TCS SP8).

Quantification of PCDPS Congeners. Concentrations of PCDPS congeners in embryos or exposure solutions were measured by use of a Trace Ultra gas chromatograph system coupled to a Trace DSQ II quadrupole mass spectrometer detector (DSQ II, Thermo Scientific, Waltham, MA) with a DB-5MS capillary column (0.25 mm × 30 m, 0.25 μm, J&K Scientific, Sunnyvale, CA). For determination of the actual waterborne concentrations, 1 mL of exposure solution of the individual PCDPS congeners from each of three replicate beakers was sampled at 21 hpf. In addition, three replicates of 30 embryos were collected at 21 hpf to determine accumulation of PCDPS congeners in developing embryos. The detailed gas chromatography−mass spectrometry analysis procedure was described previously.[11,17] Retention time, quantitative ions and recovery of each PCDPS tested are available in Supporting Information (SI) Tables S1 and S2.The limits of quantification (LOQ) were defined as ten times the ratio of signal to instrument noise (10 × S/N), that is, 0.018−0.045 ng/g wet weight and 0.015−0.032 ng/L for the PCDPSs in the biological and water samples, respectively.

Transcriptome Analysis Using RNA-seq. *RNA Preparation.* Total RNA was extracted with Trizol (Invitrogen, Burlington, ON, Canada) and genomic DNA was removed with RNase-free DNase I (Qiagen, Hilden, Germany). RNA degradation and contamination was assessed using RNase-free agarose gel electrophoresis. RNA purity (OD260/280 ratio) was determined spectrophotometrically by use of a NanoDrop 2000c (Thermo Scientific, Rockford, IL). Concentrations of RNA were measured using a Qubit 2.0 Fluorometer with a Qubit RNA XR assay kit (Invitrogen). Integrity of RNA was assessed on an Agilent 2100 Bioanalyzer with an Agilent RNA 6000 Nano Kit (Agilent Technologies, Santa Clara, CA).

Library Preparation and Sequencing. A total amount of 1 μg total RNA per sample was used to construct a library. All RNA samples had RNA integrity number scores greater than 8.2. Sequencing libraries were prepared using NEBNext Ultra II RNA Library Prep Kit for Illumina (NEB, Ipswich, MA) according to the manufacturer's instructions. Briefly, poly-A mRNA was purified from total RNA using poly-T oligo-attached magnetic beads. The extracted mRNA was chemically fragmented into RNA inserts (approximately 200 nt), which were then reverse-transcribed to first-strand cDNA using reverse transcriptase and random primers. Synthesis of second-strand cDNA was achieved using DNA Polymerase I and RNase H. After adenylation of 3′ ends of the double-stranded DNA fragments, the NEBNext Adaptor with hairpin loop structure was ligated to prepare for hybridization. In order to preferentially select cDNA fragments of 150−200 bp in length, library fragments were purified using AMPure XP system (Beckman Coulter, Beverly, MA). The size-selected fragments were then enriched via PCR and purified to produce the final cDNA library. During PCR, barcodes were incorporated by use of the NEBNext index primers, thereby enabling multiplexing. The cDNA library was analyzed on an Agilent 2100 Bioanalyzer (Agilent Technologies) to determine fragment quality and size. After cluster amplification of the cDNA libraries on a cBot Cluster Generation System using TruSeq PE Cluster Kit v3-cBot-HS (Illumina, San Diego, CA), library preparations were sequenced on an Illumina HiSeq 4000 instrument to generate 150 bp paired-end reads. All raw sequencing data were deposited at the NCBI Sequence Short Read Archive (SRA, http://www.ncbi.nlm.nih.gov/sra) under accession number SRP149041.

Bioinformatics Analysis. Clean data (clean reads) were obtained by removing adaptor sequences, poly-N and low-quality reads from the raw data. Q20, Q30, GC content, and sequence duplication level of the clean data were simultaneously calculated. All downstream analyses were based on high-quality, clean data. The paired-end clean reads were aligned to the zebrafish reference genome (Ensembl GRCz10.81) using HISAT (v2.0.4).[30] RNA transcript levels were estimated by calculating fragments per kilobase per million mapped reads (FPKM) of each gene using HTSeq v0.6.1.[31] Differential expression analysis was performed using DESeq R package (1.18.0).[32] Genes with a false discovery rate q value <0.05 were identified as DEGs. GO enrichment analysis of DEGs was performed using GOseq R package,[33] in which gene length bias was corrected. GO terms with corrected p value <0.05 were considered significantly enriched by DEGs. To identify the biological pathways involved, enrichment of DEGs in molecular pathways in the Kyoto Encyclopedia of Genes and Genomes (KEGG) was carried out using KOBAS v2.0 software.[34]

Quantitative Real-Time Polymerase Chain Reaction (qRT-PCR) Assay. For RNA-seq validation, ten genes (*mt2*, *cyp1a*, *apoea*, *hspb9*, *hspb11*, *sult6b1*, *btr30*, *egln3*, *ppp1r15a*, and *slc27a2a*) plus a reference gene, *rpl8*, were selected for

DOI: 10.1021/acs.est.8b04487
Environ. Sci. Technol. 2018, 52, 12829−12840

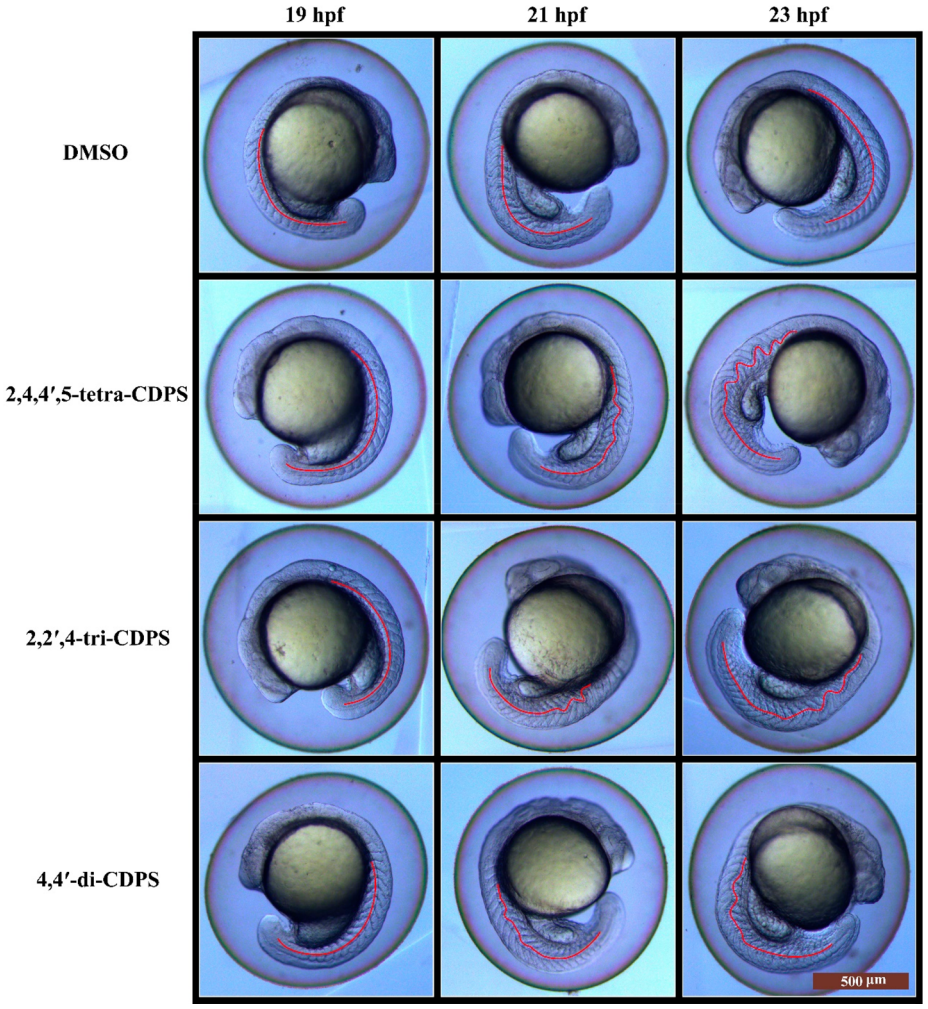

Figure 2. Representative images of developing zebrafish embryos exposed to 2500 nM 2,4,4′,5-tetra-CDPS, 2,2′,4-tri-CDPS or 4,4′-di-CDPS between 19 and 23 hpf. Notochord kinks and twists began to appear at 21 hpf for all three treatments. The notochords are marked with red curves. Scale bar: 500 μm in 70.8× magnification.

qRT-PCR analysis. The reference gene *rpl8* has previously been validated to be constantly transcribed in embryos/larvae following exposure to PCDPS congeners.[17] The PCR primer sets are available in SI Table S3. The primer sequences for *btr30* and *mt2* were designed using NCBI/Primer-BLAST software. The other primer sequences were published previously.[17,35−42] Extraction of total RNA was performed as specified in the RNA-seq experiment. A total of 1 μg of total RNA was reverse-transcribed into cDNA with PrimeScript II reverse transcriptase (Takara, Japan) in a 20-μL reaction mix, according to the manufacturer's instructions. qRT-PCR was performed on a StepOne Plus real-time PCR system (Applied Biosystems, Darmstadt, Germany) with three technical replicates for each experimental replicate. Each 20-μL reaction contained 2 μL of synthesized cDNA, 0.8 μL of 10 μmol/L forward and reverse primers, and 10 μL of 2 × SYBR Premix Ex *Taq*II (Takara). The thermal cycle profile was set at 95 °C for 30 s, followed by 40 cycles of 95 °C for 5 s and 60 °C for 30 s. Postamplification melting curve analysis was conducted to ensure the gene specificity of the primers. Raw fluorescence data were exported as clipped files and analyzed as efficiency-corrected normalized expression using LinRegPCR.[43] The relative mRNA expression of each target gene was normalized to the geometric mean of the reference gene, *rpl8*.

Synthesis and Microinjection of siRNA and mRNA. To exclude potential off-target effects of morpholino injection, the small interfering RNAs (siRNAs)-based gene-silencing strategy was chosen for knockdown of expression of specific genes in zebrafish. The siRNAs targeting zebrafish *apoea*, *hspb9* or *hspb11* transcripts and siRNA control were synthesized chemically by Integrated Biotech Solutions Company (Ibsbio, Shanghai, China) as described previously.[44] Sequences of these siRNAs are listed in SI Table S4. Full-length protein-coding sequences (CDS) of *apoea*, *hspb9* and *hspb11* were synthesized and cloned into the pcDNA3.1 (Invitrogen) vector at a position downstream of the CMV promoter by Integrated Biotech Solutions Company (SI Figure S1). The CDS incorporated the NheI restriction site sequence (GCTAGC) and a Kozak consensus sequence (GCCACCATGC) at the 5′-end and a SV40 polyadenylation signal sequence followed by a *Hin*dIII restriction site sequence (AAGCTT) at the 3′-end for directional ligation and efficient initiation of translation. All constructs were confirmed by DNA sequencing and used as templates to generate 5′-capped and 3′-poly(A)-tailed transcripts in vitro using the mMessage mMachine T7 Ultra transcription kit (Invitrogen).

Injection needles were pulled from borosilicate glass capillaries (Drummond Scientific, Broomall, PA) on a

DOI: 10.1021/acs.est.8b04487
Environ. Sci. Technol. 2018, 52, 12829−12840

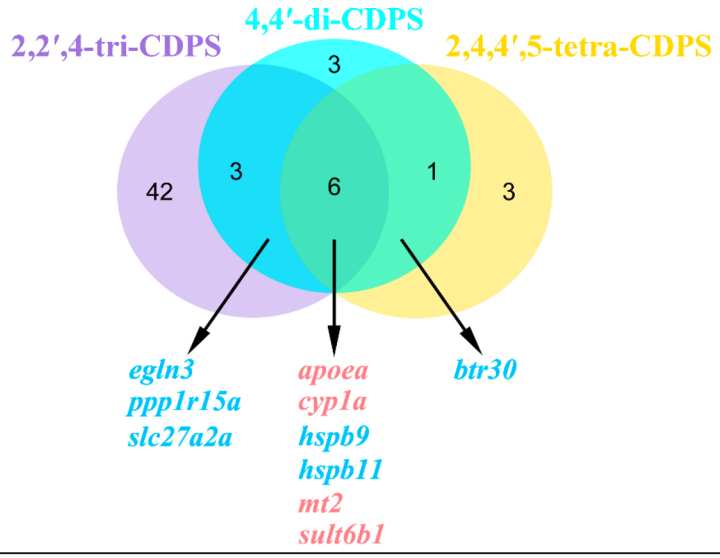

Gene	Fold change (adjusted p value)			Functional description
	2,4,4′,5-tetra-CDPS	2,2′,4-tri-CDPS	4,4′-di-CDPS	
apoea	2.06 (2.09×10^{-5})	1.79 (5.12×10^{-5})	2.18 (7.01×10^{-8})	Regulation of axon extension; Lipid transport
btr30	0.227 (1.24×10^{-3})	0.771 (1)[a]	0.216 (1.89×10^{-4})	Erythropoiesis
cyp1a	16.3 (1.82×10^{-39})	5.58 (2.15×10^{-16})	4.73 (5.48×10^{-9})	Oxidoreductase activity
egln3	0.836 (1)[a]	0.154 (3.51×10^{-5})	0.237 (8.30×10^{-3})	Angiogenesis; Neurons apoptosis
hspb11	0.555 (1.12×10^{-3})	0.607 (5.41×10^{-5})	0.567 (1.96×10^{-5})	Muscle fiber formation
hspb9	0.431 (9.75×10^{-7})	0.491 (1.01×10^{-5})	0.487 (5.89×10^{-6})	Muscle fiber formation
mt2	4.23 (2.96×10^{-13})	2.11 (2.67×10^{-7})	2.67 (1.94×10^{-10})	Angiogenesis; Metal ion binding
ppp1r15a	0.728 (1)[a]	0.428 (2.01×10^{-4})	0.484 (1.11×10^{-2})	Growth suppression and apoptosis
slc27a2a	0.971 (1)[a]	0.620 (3.51×10^{-5})	0.676 (4.18×10^{-2})	Intracellular fatty acid and lipid transport
sult6b1	2.28 (9.69×10^{-15})	1.90 (6.29×10^{-14})	1.71 (1.38×10^{-4})	Sulfotransferase activity

[a] Not identified as DEGs because the false discovery rate q value is greater or equal to 0.05.

Figure 3. Venn diagram showing differentially expressed genes in zebrafish embryos following exposure to 2500 nM 2,4,4′,5-tetra-CDPS, 2,2′,4-tri-CDPS or 4,4′-di-CDPS at 21 hpf. Up-regulated genes are highlighted in red and down-regulated genes are highlighted in blue.

horizontal bed puller (Sutter Instruments, Novato, CA). For injection, siRNA and mRNA were resuspended in DEPC-treated water. Two nL of DEPC-treated water, siRNA (100–400 pg per embryo) or mRNA (50–400 pg per embryo) were injected into the central, lower region of the first cell near the yolk-cytoplasm boundary using an Eppendorf FemtoJet microinjector (Hamburg, Germany) and a micromanipulator (MN-153, Narishige, Tokyo, Japan) under a stereomicroscope (SMZ-1000, Nikon, Tokyo, Japan). One hundred embryos were included in each injection group. Injected embryos were transferred to embryonic rearing water. Notochord morphology was observed at 21 hpf and 30 embryos were randomly sampled from each injection group, immediately frozen in liquid nitrogen, and stored at −80 °C until subsequent qRT-PCR validation.

Statistical Analysis. Before statistical procedures were applied, data were tested for normality and homogeneity of variance by a Kolmogorov–Smirnov and Levene's test using SPSS 12.0 (SPSS Inc., Chicago, IL). If normality and equal variance assumptions were met, a t test or a one-way ANOVA followed by Dunnett's test for multiple comparisons was used to identify significant embryo/larva or notochord length difference between the control and treatment groups. A value of $p < 0.05$ was considered statistically significant. When any of these assumptions were not met, the nonparametric Kruskal–Wallis test was used followed by Dunn's multiple comparison test.

RESULTS AND DISCUSSION

Exposure to PCDPSs Caused Wavy Notochord in Zebrafish Embryos at 21 hpf and Zebrafish Larvae at 120 hpf. Time-dependent morphological analysis demonstrated that exposure to each of the three individual PCDPS congeners at 2500 nM resulted in notochord kinks and twists in developing zebrafish embryos by 21 hpf (Figure 2 and SI Figure S2). The abnormal phenotype was observed in more detail by confocal laser scanning microscopy (SI Figure S3). These kinks and twists became more severe and visible at 23 hpf. Given the detection of the abnormal notochord development by 21 hpf, it was selected as the sampling and observation time point for the RNA-seq, knockdown and gain-of-function experiments, to reveal the potential molecular mechanism(s). The degree of notochord kinks and twists was different for different PCDPS treatments. 2,4,4′,5-tetra-CDPS was the most potent congener, and it induced five obvious twists in the notochord at 21 hpf. Fewer twists in notochords were observed in 2,2′,4-tri-CDPS- and 4,4′-di-CDPS- exposed embryos (4 and 3, respectively) at 21 hpf. In addition, the proportion of individuals with wavy notochord was not significantly increased at lower concentrations; however, several individuals with wavy notochord were observed. Previous chemical

DOI: 10.1021/acs.est.8b04487
Environ. Sci. Technol. 2018, 52, 12829–12840

analysis revealed that no significant degradation of PCDPSs occurred during a 24 h exposure period.[17] The actual exposure concentrations in solutions (nM) and embryos (μg/g wet weight) were measured (SI Table S5). Bioconcentration factors (BCFs), calculated for each of the three PCDPS congeners, ranged from 299 to 384 (L/kg wet weight). These values were less than values reported for exposures to lower concentrations,[17] which indicated that a higher BCF value tended to be associated with exposure to lower concentrations of PCDPSs. At 120 hpf, acute exposures to individual PCDPS congeners (dichloro- to heptachloro-diphenylsulfides) caused various malformation phenotypes (SI Figure S4) and wavy notochords were most prevalent in zebrafish larvae exposed to 2500 nM of 4,4′-di-CDPS, 2,2′,4-tri-CDPS, or 2,4,4′,5-tetra-CDPS (SI Figure S5).

Exposure to PCDPSs Altered Expression of Six Common Differentially Expressed Genes. To explore possible molecular mechanism(s) underlying the twisted and kinked notochord observed, global transcript profiles in zebrafish embryos at 21 hpf were investigated following exposure to each of the three individual PCDPS congeners (2500 nM) by use of RNA-seq All the identified DEGs are listed in SI Table S6. Due to the limited number of DEGs, no KEGG pathway was significantly enriched or modulated in the treatment groups. Significantly enriched (corrected p-value <0.05) Gene Ontology (GO) terms of development-related biological processes included lipoprotein metabolic process, lipid transport, insulin receptor signaling pathway, steroid metabolic process, negative regulation of actin nucleation, regulation of cell proliferation, and hemopoiesis.

To validate the expression profiles obtained by RNA-Seq, qRT-PCR was performed for 10 genes including *mt2*, *cyp1a*, *apoea*, *hspb9*, *hspb11*, *sult6b1*, *btr30*, *egln3*, *ppp1r15a*, and *slc27a2a*, as well as the reference gene, *rpl8*. The 10 genes were chosen based on their potential to be codifferentially expressed in at least two treatment groups. qRT-PCR results for the ten genes were generally in agreement with those determined via RNA-seq for all three PCDPSs treatment groups (SI Table S7). A linear regression analysis also revealed a significant relationship between $\log_{10}$-transformed fold-change values derived from qRT-PCR and those obtained from RNA-seq (SI Figure S6) (Pearson's $r = 0.898$, $p < 0.0001$). These results are indicative of the reliability/reproducibility of the data obtained by RNA-Seq

Among the identified DEGs, *mt2*, *cyp1a*, *apoea*, *hspb9*, *hspb11*, and *sult6b1* were significantly altered by exposure to all three individual PCDPS congeners (Figure 3). Of these, *mt2*, *cyp1a*, *apoea*, and *sult6b1* were up-regulated, and *hspb9* and *hspb11* were down-regulated. It is well-known that *cyp1a* is involved in xenobiotic metabolism.[45] Up-regulation of expression of *cyp1a* is also a well-established marker for activation of Ahr2 in zebrafish.[46] However, in zebrafish, it has been reported that dioxins cause developmental toxicities through a *cyp1a*-independent mechanism.[47] Moreover, malformation of the notochord, such as the kinks and twists observed in the present study, were not observed in zebrafish exposed to dioxin or other DLCs, which are known to bind to and activate the AHR, even though *cyp1a* was significantly up-regulated.[23,24] It has been reported that *mt2* regulates developmental angiogenesis, independent of its canonical protection function against oxidative stress or metals.[48] Up-regulation of *mt2* suggested that cardiovascular development and/or function was potentially impaired by exposure to PCDPSs through a dioxin-like mechanism.[49] The mammalian ortholog of *sult6b1* was found to encode a phase II xenobiotic-metabolizing sulfotransferase involved in the detoxification and excretion of foreign compounds.[50] Spinal curvature was observed in *hspb11* morphant zebrafish embryos,[39] which suggested a potential role of *hsps* in notochord development. Up-regulation of *apoea* was associated with growth of peripheral nervous system axons,[51] which was suspected to promote excessive growth of the notochord in PCDPS-exposed zebrafish embryos. Collectively, it was reasonably speculated that the alterations of *hspb9*, *hspb11* and *apoea* were more likely associated with the development of the wavy notochord. To examine this hypothesis, *in vivo* knockdown and gain-of-function experiments were performed in zebrafish embryos by microinjection of siRNA or mRNA.

PCDPS-Induced Wavy Notochord Was Phenocopied by Decreased Expression of *hspb9* and *hspb11* in Early Life Stages of Zebrafish Embryos. Based on the differential mRNA expression of *apoea* (up-regulation), *hspb9* (down-regulation) and *hspb11* (down-regulation), determined by RNA-Seq and qRT-PCR, *apoea* was overexpressed, and *hspb9* or *hspb11* were knocked down in vivo. Decreased expression of mRNA for *hspb9* and *hspb11* and increased expression of mRNA for *apoea* were validated by use of qRT-PCR (SI Table S8). Overexpression of *apoea* did not lead to occurrence of wavy notochord at 21 hpf (Figure 4C and D). Up-regulation of *apoea* gene might enhance neurotrophic effects on muscle to compensate for the disruption of muscle architecture,[51] which was indicated by the results of *hspb9* and *hspb11* knockdown experiments below. In addition, ApoE protein has been reported to protect cells against oxidative stress by delivering cholesterol and essential fatty acids to cells, clearing β-amyloid peptide, reducing glial cell activation, limiting glutamate excitotoxicity, and sequestering heavy metal ions.[52]

In embryos injected with 100 pg of *hspb9* siRNA (Figure 4E and F) and 400 pg of *hspb11* siRNA (Figure 4G and H), pronounced notochord kinks were detected at 21 hpf with incidences of 10% (9 of 88) and 4% (3 of 80), respectively. Although the percentages were not large, effects were sufficient to phenocopy PCDPS-induced wavy notochord. These results demonstrated that down-regulations of *hspb9* and *hspb11* were likely associated with induction of wavy notochord during zebrafish embryogenesis following exposure to PCDPS. Klüver et al. found that slow muscle myosin disorganization in skeletal muscles led to formation of gaps between slow myofibers in *hspb11* morphant zebrafish embryos.[39] Simultaneously, spinal curvature was also observed in *hspb11* morphant embryos. Another study on the mammalian ortholog of small heat shock proteins also suggested that mutation could result in desmin-related myopathy.[53] Thus, it was postulated that disruption of muscle architecture induced by knockdown of *hspb9* and *hspb11* would result in a partial loss of ability to bundle up and support the notochord, thereby resulting in wavy distortions accompanied by the initiation of spontaneous rhythmic trunk contractions[54] in embryos at 21 hpf.

Attempts were made to rescue the wavy notochord phenotype from PCDPS exposure by injection of *hspb9* or *hspb11* mRNA. Approximately 15−22% (12 of 79, 13 of 87, 14 of 65) and 7−12% (6 of 90, 7 of 71, 7 of 58) of *hspb9* or *hspb11* mRNA-injected embryos treated with 4,4′-di-CDPS, 2,2′,4-tri-CDPS or 2,4,4′,5-tetra-CDPS exhibited a rescued notochord phenotype at 21 hpf (SI Figure S7). These results indicated that restored expression of *hspb9* or *hspb11* in

DOI: 10.1021/acs.est.8b04487
Environ. Sci. Technol. 2018, 52, 12829−12840

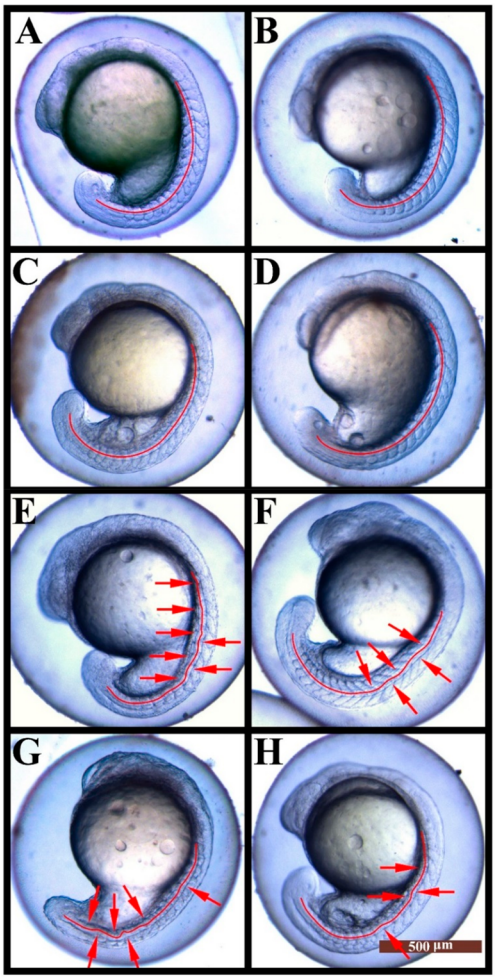

Figure 4. Knockdown of *hspb9* and *hspb11* results in strikingly wavy notochords. Phenotypic observations of embryos microinjected with 2 nL of DEPC-treated water (A), 400 pg of siRNA negative control (B), 400 pg of 5′-capped and 3′-polyadenylated transcripts encoding ApoEa (C and D), 100 pg of *hspb9* siRNA (E and F), and 400 pg of *hspb11* siRNA (G and H) at 21 hpf. The notochords are marked with red curves. The arrows indicate multiple kinks caused by siRNA-mediated transcriptional gene silencing of *hspb9* or *hspb11* (E–H). Scale bar: 500 μm in 70.8× magnification.

PCDPS-treated embryos prevented the wavy notochord phenotype, although rates of rescue were low. The low responses of siRNA knockdown experiments and the rescue experiments might be because the injected siRNA or mRNA did not enter the notochord and surrounding muscles in some developing embryos, or levels of expression of mRNA or protein varied among individuals. In addition, the sum of rescue percentages (14%) in our study was comparable with the 14% for *sox9b* mRNA-rescued jaw malformation induced by TCDD reported previously.[26] Overall, these results support the hypothesis that PCDPS-induced wavy notochord in early life stages of zebrafish embryos is related, at least in part, to the suppressed expression of *hspb9* or *hspb11*. Certainly, there is a possibility that wavy notochord is mediated by some other unknown mechanism(s), which deserves further investigation in future studies.

Body Growth Retardation Accompanied with Normal Extension of Notochord Intensified the Level of Notochord Kinks and Twists. No significant difference was observed in notochord length between the control and PCDPS treatments at 21 or 120 hpf (Figure 5). However, the ratio of notochord length to embryo/larva length, which was

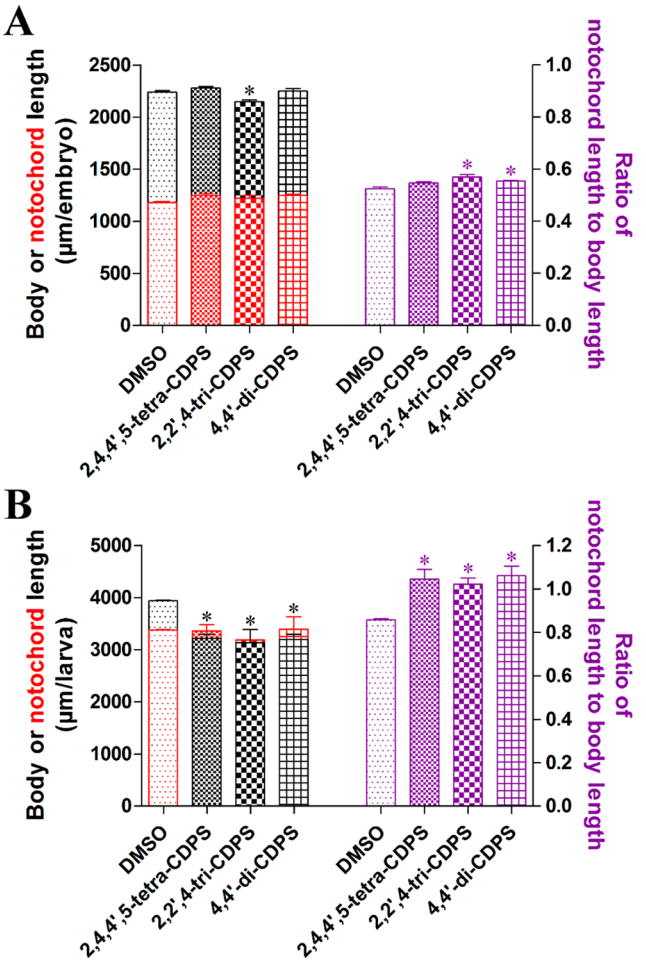

Figure 5. Embryo/larva and notochord length, and the ratio of notochord length to embryo/larva length at 21 hpf (A) and 120 hpf (B). Black columns represent embryo/larva lengths and the red represent notochord lengths. Purple columns represent the ratio of notochord length to embryo/larva length.

used to semiquantitatively characterize the level of notochord kinks and twists, was significantly greater in embryos/larvae exposed to each of the three PCDPS congeners at 21 and 120 hpf compared with the control (exception was 2,4,4′,5-tetra-CDPS-exposed embryos at 21 hpf; however, an increasing trend was observed). At 21 hpf, body axis elongation was inhibited only in embryos exposed to 2,2′,4-tri-CDPS. The results indicated that the notochord kinks and twists were not likely triggered by a reduction in embryo length. As exposure and development progressed, the reduction of body length became more pronounced and significant for exposures to all three PCDPSs at 120 hpf, which resulted in notochord to larval length ratios exceeding one. These results indicated that retardation of body growth intensified the level of notochord kinks and twists caused by exposure to PCDPS. PCDPS exposure seemed to preferentially disrupt body axis elongation but not notochord extension. This may be driven by differences in response to the cellular origins of the muscle and notochord, i.e. myotomes and sclerotomes, respectively. In addition, normal notochord length might also be associated with up-regulation of *apoea*, which could promote growth of

DOI: 10.1021/acs.est.8b04487
Environ. Sci. Technol. 2018, 52, 12829−12840

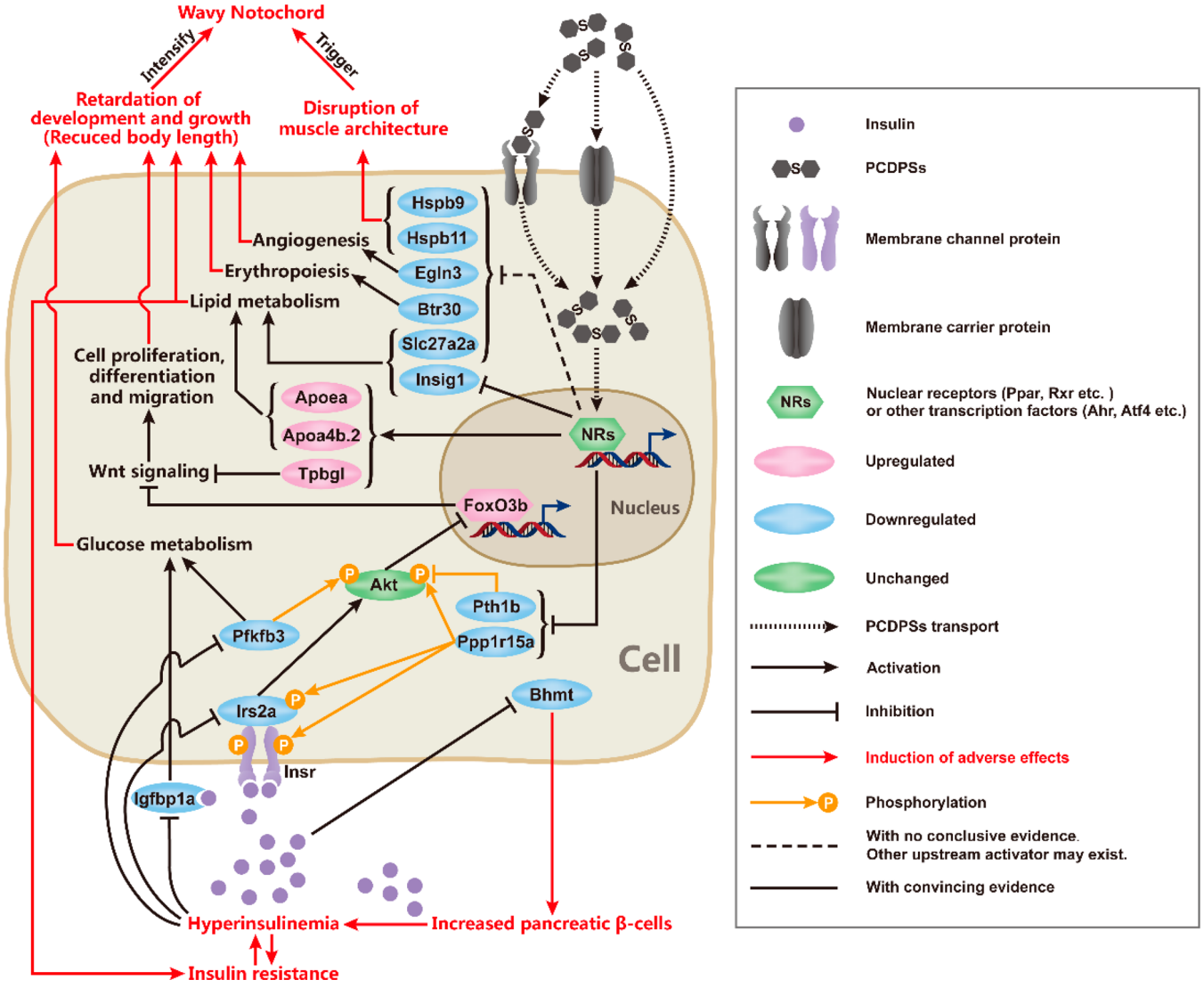

Figure 6. Schematic representation of the possible mechanisms underlying PCDPSs-induced wavy notochord.

notochord as well as peripheral nervous system axons,[51] thereby providing protective effects against PCDPS-induced retardation of extension growth in PCDPS-exposed zebrafish embryos.

Dysregulation of Genes Involved in Embryonic Development and Growth May Be Related to the Reduction of Embryo/Larva Lengths. It is worth mentioning that, at 21 hpf, lengths of embryos were significantly reduced only in embryos exposed to 2,2′,4-tri-CDPS, which might explain why the ratio of notochord length to embryo length was greater than those for the other two PCDPS-treated groups. The significant body growth retardation might be related to altered expression of genes regulating embryonic development and growth. Among the 42 genes differentially expressed only in 21-hpf embryos exposed to 2,2′,4-tri-CDPS (SI Table S6), 8, including *foxo3b*, *tpbgl*, *irs2a*, *insig1*, *bhmt*, *igfbp1a*, *pfkfb3*, and *pth1b*, are involved in embryonic development and growth (Figure 6). Two of the genes, *foxo3b* and *tpbgl*, were significantly up-regulated, while the remaining 6, *irs2a*, *insig1*, *bhmt*, *igfbp1a*, *pfkfb3*, and *pth1b*, were significantly down-regulated. Mechanistically, exposure to 2,2′,4-tri-CDPS might lead to the occurrence of insulin resistance, similar to findings by Ruzzin et al. demonstrating that exposure to other POPs, including dichlorodiphenyltrichloroethane (DDT), PCDDs/Fs and PCBs, led to insulin resistance syndrome.[55] Dysregulation of *apoea* and *insig1*, two major regulators of triglyceride and cholesterol biosynthesis, could cause disruption of metabolism of lipids[52,56] and contribute to development of insulin resistance and hyperinsulinemia.[57−59] High levels of insulin decreased abundance of *bhmt* mRNA and the rate of de novo mRNA transcription of the gene,[60] thereby resulting in a possible compensatory increase in the number of *β*-cells in pancreatic islets.[61] This would contribute to a potential further increase in insulin levels. Hyperinsulinemia also inhibited transcription of *igfbp1a* and *pfkfb3*, which are involved in glucose metabolism during embryonic growth.[62,63] In addition, insulin could cause internalization of insulin receptors (Insr), followed by degradation or inactivation, which could subsequently lead to decreased transcription of *irs2a* under conditions of insulin resistance.[64] *Pfkfb3* positively regulates insulin-stimulated Akt signaling via phosphorylation of Akt.[65] Irs2 also functions as a positive regulator of insulin signaling through the Insr/Irs/Phosphatidylinositol 3-Kinase/Akt cascade,[66] whereas the Pth family of hormones suppresses insulin signaling via reducing phosphorylation of Akt.[67] The consequent decreased phos-

DOI: 10.1021/acs.est.8b04487
Environ. Sci. Technol. 2018, 52, 12829−12840

phorylation of Akt lessened inhibition of Akt on FoxO3b transcription factor.[68] FoxO3b and Tpbgl (also known as Wnt-activated inhibitory factors) negatively regulate Wnt signaling,[69,70] thus transcriptional up-regulation of *foxo3b* and *tpbgl*, observed in the present study, was speculated to inhibit downstream Wnt signaling. It is known that Wnt signaling plays a critical role in embryonic development and growth through proper regulation of cell proliferation,[71] differentiation[72] and migration.[73] Thus, exposure to 2,2′,4-tri-CDPS altered expression of mRNA of more genes involved in the insulin-associated Irs−Akt−FoxO cascade compared with the other two PCDPS congeners. Such effects on this cascade could lead to insulin resistance syndrome-associated metabolic disorders and eventually the significant reduction of embryo lengths reported at 21 hpf. In 21-hpf zebrafish embryos exposed to 2,4,4′,5-tetra-CDPS or 4,4′-di-CDPS, expression profiles of mRNA were consistent with those in zebrafish embryos exposed to 2,2′,4-tri-CDPS for the insulin resistance-associated genes mentioned above. This indicated that insulin resistance syndrome-associated metabolic disorders could also be present in zebrafish embryos exposed to 2,4,4′,5-tetra-CDPS or 4,4′-di-CDPS. In-depth studies, such as measurement of Akt expression/phosphorylation, expression of inhibitor cytokines targeting Jak/Stat signaling, and glucose tolerance, are necessary to definitively demonstrate the hypothesis of insulin resistance. Unfortunately, it is difficult to do these studies at such an early embryonic stage currently. However, as we know, 21-hpf zebrafish have an undifferentiated pancreas and a possible primordial liver bud (24−50 hpf),[74] which are both major components of insulin signaling.[75,76] Gene *pancreaticandduodenalhomeobox1* is first detected at the 10-somite stage (∼14 hpf), which indicates the earliest appearance of pancreatic precursors.[76] As development progresses, a dorsal pancreatic bud begins to express insulin at the 12-somite stage (∼15 hpf).[76] In addition, the earliest liver differentiation marker thus far described in zebrafish, *ceruloplasmin*, is detected in the dorsal endoderm at 16 hpf and in the early hepatic cells in the yolk sac at 24 hpf.[74] Take together, these findings suggested that insulin signaling was really likely involved with somatic growth at 21 hpf.

Additional genes associated with embryonic development and growth were significantly codown-regulated following 2,2′,4-tri-CDPS and 4,4′-di-CDPS exposure (*egln3*, *ppp1r15a* and *slc27a2a*) and 2,4,4′,5-tetra-CDPS and 4,4′-di-CDPS exposure (*btr30*). Previous studies demonstrated that down-regulation of *egln3*, also termed *prolyl hydroxylase 3*, was associated with abnormal development of blood vessels in zebrafish embryos in a Hif-dependent manner[77] and promoted apoptosis in a Hif-independent manner in both peripheral and central neurons.[78,79] The mammalian ortholog of *ppp1r15a* was correlated with growth suppression and apoptosis through modulating phosphatase activity.[80] As a fatty acid transporter, *slc27a2a* is involved in intracellular transport of fatty acids and lipids.[81] Finally, *btr30* is inferred to be involved in erythropoiesis in zebrafish.[82] Overall, based on the mRNA expression results, reduction of embryo/larva lengths might be partly attributed to dysregulation of genes involved in insulin signaling, thereby potentially leading to retardation of embryonic development and growth. To facilitate understanding of this proposed possible mechanism underlying the development of wavy notochord in early life stages of zebrafish following exposure to PCDPS congeners, a schematic representation is provided (Figure 6).

Exposure to dithiocarbamate (DTC) pesticides, including tetramethylthiuram disulfide (thiram), zinc dimethyldithiocarbamate (ziram), and sodium metam (NaM),[83] was shown to cause a wavy distortion of the notochord—similar to PCDPSs in this study—in zebrafish from 4 to 24 hpf with EC_{50} values of 7, 26, and 300 nM for thiram, ziram and NaM, respectively.[54,84] Existing studies show that the common molecular mechanism for DTCs is different from that of PCDPSs. Disruption of *collagen 2a1* expression was found in DTC-exposed zebrafish embryos, which infers that DTCs may perturb early developmental processes related to collagen formation and somitogenesis,[84,85] thereby impairing trunk plasticity and resulting in the wavy distortion of the notochord with the onset of spontaneous rhythmic trunk contractions.[54]

In summary, the results of this study support the hypothesis that down-regulation of *hspb9* and *hspb11* plays a role in development of wavy notochord in early life stages of zebrafish. Suppressed expression of *hspb9* and *hspb11* was postulated to cause disruption of muscle architecture followed by a partial loss of ability to bundle up and support the notochord leading to wavy distortions. These effects were suggested to be accompanied by initiation of spontaneous rhythmic trunk contractions in embryos at 21 hpf. In addition, dysregulation of several genes involved in the insulin-associated Irs-Akt-FoxO cascade was proposed to explain the inhibition of body axis elongation. Given that notochord growth was not affected, the resulting compression force would result in more severe and pronounced notochord kinks and twists as exposure and development progressed. To our knowledge, this is the first report revealing the potential molecular mechanism underlying the wavy notochord phenotype induced by the emerging DLCs, PCDPSs, in early life stages of zebrafish. Furthermore, these effects of PCDPS provide novel insights into molecular mechanisms—possibly downstream of Ahr2 or other nuclear receptors/transcription factors—of dioxins/DLCs-induced teratogenicity and developmental toxicity in early life stages of vertebrates. Concentrations of PCDPS congeners used in the present study, whereas several orders of magnitude higher than those detected in surface waters, permitted the elucidation of potential mechanisms that could lead to effects in more sensitive species under field conditions. Given the possibility of areas that are highly contaminated with PCDPSs due to their widespread production and use, and the potential for PCDPSs to bioaccumulate and biomagnify through the food chain, further research to evaluate impacts on wildlife and human health, especially in early life stages is warranted. Finally, our findings provide experimental evidence to support the notion that elevated body burdens of POPs are potential contributors to the development of the worldwide prevalence of insulin resistance and associated disorders, which is often observed in obese and diabetic individuals and in individuals affected by metabolic syndrome.

■ ASSOCIATED CONTENT

Supporting Information

The Supporting Information is available free of charge on the ACS Publications website at DOI: 10.1021/acs.est.8b04487.

Plasmid maps and sequences of plasmid constructs (Figure S1); time-course morphological changes of PCDPS-exposed zebrafish embryos (Figure S2); representative confocal micrographs of notochord at 21 hpf (Figure S3); representative optical images of deformed

DOI: 10.1021/acs.est.8b04487
Environ. Sci. Technol. 2018, 52, 12829−12840

zebrafish larvae (Figure S4) and wavy notochord (Figure S5) at 120 hpf; linear regression analysis comparing log_{10}-transformed fold-change values derived from qRT-PCR with those obtained from RNA-seq (Figure S6); representative images of rescued notochord phenotypes (Figure S7); quantification of PCDPS congeners in exposure solutions and zebrafish embryos/larvae (Tables S1, S2 and S5); primer sequences of the selected differentially expressed genes and reference gene (*rpl8*) in zebrafish for qRT-PCR (Table S3); sequences of siRNA oligo-duplexes (Table S4); detailed information on differentially expressed genes (Table S6); fold change of target mRNA in zebrafish embryos exposed to PCDPS congeners (Table S7) or injected with siRNA or mRNA (Table S8) (PDF)

AUTHOR INFORMATION

Corresponding Author

*Phone: 86 27 87282113; fax: 86 27 87282114; e-mail: cliu@mail.hzau.edu.cn.

ORCID

Doug Crump: 0000-0003-2915-4989

Robert J. Letcher: 0000-0002-8232-8565

Chunsheng Liu: 0000-0002-9206-9894

Notes

The authors declare no competing financial interest.

ACKNOWLEDGMENTS

This work was financially supported by the National Natural Science Foundation of China (No. 21607001 and 21622702), the Anhui Provincial Natural Science Foundation (No. 1608085QB45), and the Science Research Project of Anhui Education Department (No. KJ2015A090). X.W. acknowledges the support from the China Scholarship Council (CSC, 201406190170). J.P.G. was supported by the Canada research Chairs program of the Natural Science and Engineering Council of Canada.

REFERENCES

(1) Nakanishi, H.; Umemoto, N. Thermal-resistant lubricating oil composition for gas turbines or jet engines. 13, JP 2002003878 A. 2002.

(2) Munch, R. H.; Thompson, Q. E. Electrical devices containing readily biodegradable dielectric fluids. 29, CA 1081937, 1980.

(3) Dorweiler, K. J.; Gurav, J. N.; Walbridge, J. S.; Ghatge, V. S.; Savant, R. H. Determination of stability from multicomponent pesticide mixes. *J. Agric. Food Chem.* **2016**, *64* (31), 6108−6124.

(4) Fan, C. L.; Li, Y.; Chang, Q. Y.; Pang, G. F.; Kang, J.; Cao, J.; Zhao, Y. B.; Li, N.; Li, Z. Y. High-throughput analytical techniques for multiresidue, multiclass determination of 653 pesticides and chemical pollutants in tea−Part IV: Evaluation of the ruggedness of the method, error analysis, and key control points of the method. *J. AOAC Int.* **2015**, *98* (1), 130−148.

(5) Mitchell, L. R. Collaborative study of the determination of endosulfan, endosulfan sulfate, tetrasul, and tetradifon residues in fresh fruits and vegetables. *J. Assoc. Off. Anal. Chem.* **1976**, *59* (1), 209−212.

(6) Pscheidt, J. W.; Peachey, R. E.; Castagnoli, S. *2015 Peach Pest Management Guide for Oregon*; Extension Service, Oregon State University: Corvallis, OR, 2015.

(7) Yang, X.; Zhang, H.; Liu, Y.; Wang, J.; Zhang, Y. C.; Dong, A. J.; Zhao, H. T.; Sun, C. H.; Cui, J. Multiresidue method for determination of 88 pesticides in berry fruits using solid-phase extraction and gas chromatography−mass spectrometry: determination of 88 pesticides in berries using SPE and GC−MS. *Food Chem.* **2011**, *127* (2), 855−865.

(8) Sinkkonen, S.; Kolehmalnen, E.; Laihia, K.; Koistinen, J.; Rantio, T. Polychlorinated diphenyl sulfides: preparation of model compounds, chromatography, mass spectrometry, NMR, and environmental analysis. *Environ. Sci. Technol.* **1993**, *27* (7), 1319−1326.

(9) Sinkkonen, S.; Vattulainen, A.; Aittola, J. P.; Paasivirta, J.; Tarhanen, J.; Lahtiperä, M. Metal reclamation produces sulphur analogues of toxic dioxins and furans. *Chemosphere* **1994**, *28* (7), 1279−1288.

(10) Schwarzbauer, J.; Littke, R.; Weigelt, V. Identification of specific organic contaminants for estimating the contribution of the Elbe river to the pollution of the German Bight. *Org. Geochem.* **2000**, *31* (12), 1713−1731.

(11) Zhang, X.; Qin, L.; Qu, R.; Feng, M.; Wei, Z.; Wang, L.; Wang, Z. Occurrence of polychlorinated diphenyl sulfides (PCDPSs) in surface sediments and surface water from the Nanjing section of the Yangtze River. *Environ. Sci. Technol.* **2014**, *48* (19), 11429−11436.

(12) de Tonkelaar, E. M.; van Esch, G. J. No-effect levels organochlorine pesticides based on induction of microsomal liver enzymes in short-term toxicity experiments. *Toxicology* **1974**, *2* (4), 371−380.

(13) Li, Y.; Li, M.; Shi, J.; Yang, X.; Wang, Z. Hepatic antioxidative responses to PCDPSs and estimated short-term biotoxicity in freshwater fish. *Aquat. Toxicol.* **2012**, *120−121*, 90−98.

(14) Zhang, X.; Liu, F.; Chen, B.; Li, Y.; Wang, Z. Acute and subacute oral toxicity of polychlorinated diphenyl sulfides in mice: determining LD_{50} and assessing the status of hepatic oxidative stress. *Environ. Toxicol. Chem.* **2012**, *31* (7), 1485−1493.

(15) Verschuuren, H. G.; Kroes, R.; Van Esch, G. J. Toxicity studies on tetrasul I. Acute, long-term and reproduction studies. *Toxicology* **1973**, *1* (1), 63−78.

(16) Smyth, H. F.; Carpenter, C. P.; Well, C. S.; Pozzani, U. C.; Striegel, J. A. Range-finding toxicity data: List VI. *Am. Ind. Hyg. Assoc. J.* **1962**, *23* (2), 95−107.

(17) Zhang, R.; Wang, X.; Zhang, X.; Song, C.; Letcher, R. J.; Liu, C. Polychlorinated diphenylsulfides activate aryl hydrocarbon receptor 2 in zebrafish embryos: potential mechanism of developmental toxicity. *Environ. Sci. Technol.* **2018**, *52* (7), 4402−4412.

(18) Zhang, J.; Zhang, X.; Xia, P.; Zhang, R.; Wu, Y.; Xia, J.; Su, G.; Zhang, J.; Giesy, J. P.; Wang, Z.; Villeneuve, D. L.; Yu, H. Activation of AhR-mediated toxicity pathway by emerging pollutants polychlorinated diphenyl sulfides. *Chemosphere* **2016**, *144* (Supplement C), 1754−1762.

(19) Zhang, R.; Zhang, X.; Zhang, J.; Qu, R.; Zhang, J.; Liu, X.; Chen, J.; Wang, Z.; Yu, H. Activation of avian aryl hydrocarbon receptor and inter-species sensitivity variations by polychlorinated diphenylsulfides. *Environ. Sci. Technol.* **2014**, *48* (18), 10948−10956.

(20) Mostrag, A.; Puzyn, T.; Haranczyk, M. Modeling the overall persistence and environmental mobility of sulfur-containing polychlorinated organic compounds. *Environ. Sci. Pollut. Res.* **2010**, *17* (2), 470−477.

(21) Zhang, X.; Fang, B.; Wang, T.; Liu, H.; Feng, M.; Qin, L.; Zhang, R. Tissue-specific bioaccumulation, depuration and metabolism of 4,4′-dichlorodiphenyl sulfide in the freshwater mussel *Anodonta woodiana*. *Sci. Total Environ.* **2018**, *642*, 854−863.

(22) Shi, J.; Zhang, X.; Qu, R.; Xu, Y.; Wang, Z. Synthesis and QSPR study on environment-related properties of polychlorinated diphenyl sulfides (PCDPSs). *Chemosphere* **2012**, *88* (7), 844−854.

(23) Marit, J. S.; Weber, L. P. Persistent effects on adult swim performance and energetics in zebrafish developmentally exposed to 2,3,7,8-tetrachlorodibenzo-*p*-dioxin. *Aquat. Toxicol.* **2012**, *106−107*, 131−139.

(24) Andreasen, E. A.; Spitsbergen, J. M.; Tanguay, R. L.; Stegeman, J. J.; Heideman, W.; Peterson, R. E. Tissue-specific expression of AHR2, ARNT2, and CYP1A in zebrafish embryos and larvae: effects of developmental stage and 2,3,7,8-tetrachlorodibenzo-*p*-dioxin exposure. *Toxicol. Sci.* **2002**, *68* (2), 403−419.

DOI: 10.1021/acs.est.8b04487
Environ. Sci. Technol. 2018, 52, 12829−12840

(25) McMillan, B. J.; Bradfield, C. A. The aryl hydrocarbon receptor sans xenobiotics: endogenous function in genetic model systems. *Mol. Pharmacol.* **2007**, *72* (3), 487−498.
(26) Xiong, K. M.; Peterson, R. E.; Heideman, W. Aryl hydrocarbon receptor-mediated down-regulation of *sox9b* causes jaw malformation in zebrafish embryos. *Mol. Pharmacol.* **2008**, *74* (6), 1544−1553.
(27) Zhang, X.; Shi, J.; Sun, L.; Wang, Z. Palladium-catalyzed carbon-sulfur bond formation to synthesize polychlorinated diphenyl sulfides. *Org. Chem. Front.* **2011**, *31* (7), 1107−1113.
(28) Amsterdam, A.; Nissen, R. M.; Sun, Z.; Swindell, E. C.; Farrington, S.; Hopkins, N. Identification of 315 genes essential for early zebrafish development. *Proc. Natl. Acad. Sci. U. S. A.* **2004**, *101* (35), 12792−12797.
(29) Abràmoff, M. D.; Magalhães, P. J.; Ram, S. J. Image processing with ImageJ. *Biophotonics International* **2004**, *11* (7), 36−42.
(30) Kim, D.; Langmead, B.; Salzberg, S. L. HISAT: a fast spliced aligner with low memory requirements. *Nat. Methods* **2015**, *12*, 357.
(31) Anders, S.; Pyl, P. T.; Huber, W. HTSeq−a Python framework to work with high-throughput sequencing data. *Bioinformatics* **2015**, *31* (2), 166−169.
(32) Anders, S.; Huber, W. Differential expression analysis for sequence count data. *Genome Biol.* **2010**, *11* (10), R106.
(33) Young, M. D.; Wakefield, M. J.; Smyth, G. K.; Oshlack, A. Gene ontology analysis for RNA-seq: accounting for selection bias. *Genome Biol.* **2010**, *11* (2), R14.
(34) Mao, X.; Cai, T.; Olyarchuk, J. G.; Wei, L. Automated genome annotation and pathway identification using the KEGG Orthology (KO) as a controlled vocabulary. *Bioinformatics* **2005**, *21* (19), 3787−3793.
(35) Lee, J.; Peterson, S. M.; Freeman, J. L. Sex-specific characterization and evaluation of the Alzheimer's disease genetic risk factor sorl1 in zebrafish during aging and in the adult brain following a 100 ppb embryonic lead exposure. *J. Appl. Toxicol.* **2017**, *37* (4), 400−407.
(36) Kühnert, A.; Vogs, C.; Seiwert, B.; Aulhorn, S.; Altenburger, R.; Hollert, H.; Küster, E.; Busch, W. Biotransformation in the zebrafish embryo−temporal gene transcription changes of cytochrome P450 enzymes and internal exposure dynamics of the AhR binding xenobiotic benz[a]anthracene. *Environ. Pollut.* **2017**, *230*, 1−11.
(37) Manchenkov, T.; Pasillas, M. P.; Haddad, G. G.; Imam, F. B. Novel genes critical for hypoxic preconditioning in zebrafish are regulators of insulin and glucose metabolism. *G3: Genes, Genomes, Genet.* **2015**, *5* (6), 1107−1116.
(38) Elicker, K. S.; Hutson, L. D. Genome-wide analysis and expression profiling of the small heat shock proteins in zebrafish. *Gene* **2007**, *403* (1), 60−69.
(39) Klüver, N.; Yang, L.; Busch, W.; Scheffler, K.; Renner, P.; Strähle, U.; Scholz, S. Transcriptional response of zebrafish embryos exposed to neurotoxic compounds reveals a muscle activity dependent hspb11 expression. *PLoS One* **2011**, *6* (12), e29063.
(40) Ho, N. Y.; Yang, L.; Legradi, J.; Armant, O.; Takamiya, M.; Rastegar, S.; Strähle, U. Gene responses in the central nervous system of zebrafish embryos exposed to the neurotoxicant methyl mercury. *Environ. Sci. Technol.* **2013**, *47* (7), 3316−3325.
(41) Zheng, W.; Li, Z.; Nguyen, A. T.; Li, C.; Emelyanov, A.; Gong, Z. Xmrk, Kras and Myc transgenic zebrafish liver cancer models share molecular signatures with subsets of human hepatocellular carcinoma. *PLoS One* **2014**, *9* (3), e91179.
(42) Pradhan, A.; Ivarsson, P.; Ragnvaldsson, D.; Berg, H.; Jass, J.; Olsson, P. E. Transcriptional responses of zebrafish to complex metal mixtures in laboratory studies overestimates the responses observed with environmental water. *Sci. Total Environ.* **2017**, *584−585*, 1138−1146.
(43) Ruijter, J. M.; Ramakers, C.; Hoogaars, W. M. H.; Karlen, Y.; Bakker, O.; van den Hoff, M. J. B.; Moorman, A. F. M. Amplification efficiency: linking baseline and bias in the analysis of quantitative PCR data. *Nucleic Acids Res.* **2009**, *37* (6), e45−e45.
(44) Donzé, O.; Picard, D. RNA interference in mammalian cells using siRNAs synthesized with T7 RNA polymerase. *Nucleic Acids Res.* **2002**, *30* (10), e46−e46.
(45) Miranda, C. L.; Chung, W. G.; Wang-Buhler, J. L.; Musafia-Jeknic, T.; Baird, W. M.; Buhler, D. R. Comparative in vitro metabolism of benzo[a]pyrene by recombinant zebrafish CYP1A and liver microsomes from β-naphthoflavone-treated rainbow trout. *Aquat. Toxicol.* **2006**, *80* (2), 101−108.
(46) Denison, M. S.; Fisher, J. M.; Whitlock, J. P. Inducible, receptor-dependent protein-DNA interactions at a dioxin-responsive transcriptional enhancer. *Proc. Natl. Acad. Sci. U. S. A.* **1988**, *85* (8), 2528−2532.
(47) Carney, S. A.; Peterson, R. E.; Heideman, W. 2,3,7,8-Tetrachlorodibenzo-*p*-dioxin activation of the aryl hydrocarbon receptor/aryl hydrocarbon receptor nuclear translocator pathway causes developmental toxicity through a CYP1A-independent mechanism in zebrafish. *Mol. Pharmacol.* **2004**, *66* (3), 512−521.
(48) Schuermann, A.; Helker, C. S. M.; Herzog, W. Metallothionein 2 regulates endothelial cell migration through transcriptional regulation of vegfc expression. *Angiogenesis* **2015**, *18* (4), 463−475.
(49) Carney, S. A.; Prasch, A. L.; Heideman, W.; Peterson, R. E. Understanding dioxin developmental toxicity using the zebrafish model. *Birth Defects Res., Part A* **2006**, *76* (1), 7−18.
(50) Takahashi, S.; Sakakibara, Y.; Mishiro, E.; Kouriki, H.; Nobe, R.; Kurogi, K.; Yasuda, S.; Liu, M. C.; Suiko, M. Molecular cloning, expression and characterization of a novel mouse SULT6 cytosolic sulfotransferase. *J. Biochem.* **2009**, *146* (3), 399−405.
(51) Ignatius, M. J.; Gebicke-Härter, P. J.; Skene, J. H.; Schilling, J. W.; Weisgraber, K. H.; Mahley, R. W.; Shooter, E. M. Expression of apolipoprotein E during nerve degeneration and regeneration. *Proc. Natl. Acad. Sci. U. S. A.* **1986**, *83* (4), 1125−1129.
(52) Lane, R. M.; Farlow, M. R. Lipid homeostasis and apolipoprotein E in the development and progression of Alzheimer's disease. *J. Lipid Res.* **2005**, *46* (5), 949−968.
(53) Vicart, P.; Caron, A.; Guicheney, P.; Li, Z.; Prévost, M. C.; Faure, A.; Chateau, D.; Chapon, F.; Tomé, F.; Dupret, J. M.; Paulin, D.; Fardeau, M. A missense mutation in the αB-Crystallin chaperone gene causes a desmin-related myopathy. *Nat. Genet.* **1998**, *20*, 92.
(54) Teraoka, H.; Urakawa, S.; Nanba, S.; Nagai, Y.; Dong, W.; Imagawa, T.; Tanguay, R. L.; Svoboda, K.; Handley-Goldstone, H. M.; Stegeman, J. J.; Hiraga, T. Muscular contractions in the zebrafish embryo are necessary to reveal thiuram-induced notochord distortions. *Toxicol. Appl. Pharmacol.* **2006**, *212* (1), 24−34.
(55) Ruzzin, J.; Petersen, R.; Meugnier, E.; Madsen, L.; Lock, E. J.; Lillefosse, H.; Ma, T.; Pesenti, S.; Sonne, S. B.; Marstrand, T. T.; Malde, M. K.; Du, Z. Y.; Chavey, C.; Fajas, L.; Lundebye, A. K.; Brand, C. L.; Vidal, H.; Kristiansen, K.; Frøyland, L. Persistent organic pollutant exposure leads to insulin resistance syndrome. *Environ. Health Perspect.* **2010**, *118* (4), 465−471.
(56) Smith, E. M.; Zhang, Y.; Baye, T. M.; Gawrieh, S.; Cole, R.; Blangero, J.; Carless, M. A.; Curran, J. E.; Dyer, T. D.; Abraham, L. J.; Moses, E. K.; Kissebah, A. H.; Martin, L. J.; Olivier, M. INSIG1 influences obesity-related hypertriglyceridemia in humans. *J. Lipid Res.* **2010**, *51* (4), 701−708.
(57) Roden, M.; Price, T. B.; Perseghin, G.; Petersen, K. F.; Rothman, D. L.; Cline, G. W.; Shulman, G. I. Mechanism of free fatty acid-induced insulin resistance in humans. *J. Clin. Invest.* **1996**, *97* (12), 2859−2865.
(58) Koyama, K.; Chen, G.; Lee, Y.; Unger, R. H. Tissue triglycerides, insulin resistance, and insulin production: implications for hyperinsulinemia of obesity. *Am. J. Physiol.-Endocrinol. Metab.* **1997**, *273* (4), E708−E713.
(59) Shanik, M. H.; Xu, Y.; Škrha, J.; Dankner, R.; Zick, Y.; Roth, J. Insulin resistance and hyperinsulinemia: is hyperinsulinemia the cart or the horse? *Diabetes Care* **2008**, *31* (Supplement 2), S262−S268.
(60) Yang, S. L.; Aw, S. S.; Chang, C.; Korzh, S.; Korzh, V.; Peng, J. Depletion of Bhmt elevates sonic hedgehog transcript level and increases β-cell number in zebrafish. *Endocrinology* **2011**, *152* (12), 4706−4717.

DOI: 10.1021/acs.est.8b04487
Environ. Sci. Technol. 2018, 52, 12829−12840

(61) Ratnam, S.; Wijekoon, E. P.; Hall, B.; Garrow, T. A.; Brosnan, M. E.; Brosnan, J. T. Effects of diabetes and insulin on betaine-homocysteine S-methyltransferase expression in rat liver. *Am. J. Physiol.-Endocrinol. Metab.* **2006**, *290* (5), E933−E939.
(62) Lee, P. D. K.; Giudice, L. C.; Conover, C. A.; Powell, D. R. Insulin-like growth factor binding protein-1: recent findings and new directions. *Exp. Biol. Med.* **1997**, *216* (3), 319−357.
(63) Atsumi, T.; Nishio, T.; Niwa, H.; Takeuchi, J.; Bando, H.; Shimizu, C.; Yoshioka, N.; Bucala, R.; Koike, T. Expression of inducible 6-phosphofructo-2-kinase/fructose-2, 6-bisphosphatase/PFKFB3 isoforms in adipocytes and their potential role in glycolytic regulation. *Diabetes* **2005**, *54* (12), 3349−3357.
(64) Green, A.; Olefsky, J. M. Evidence for insulin-induced internalization and degradation of insulin receptors in rat adipocytes. *Proc. Natl. Acad. Sci. U. S. A.* **1982**, *79* (2), 427−431.
(65) Trefely, S.; Khoo, P. S.; Krycer, J. R.; Chaudhuri, R.; Fazakerley, D. J.; Parker, B. L.; Sultani, G.; Lee, J.; Stephan, J. P.; Torres, E.; Jung, K.; Kuijl, C.; James, D. E.; Junutula, J. R.; Stöckli, J. Kinome screen identifies PFKFB3 and glucose metabolism as important regulators of the insulin/insulin-like growth factor (IGF)-1 signaling pathway. *J. Biol. Chem.* **2015**, *290* (43), 25834−25846.
(66) Wick, K. R.; Werner, E. D.; Langlais, P.; Ramos, F. J.; Dong, L. Q.; Shoelson, S. E.; Liu, F. Grb10 inhibits insulin-stimulated insulin receptor substrate (IRS)-phosphatidylinositol 3-kinase/Akt signaling pathway by disrupting the association of IRS-1/IRS-2 with the insulin receptor. *J. Biol. Chem.* **2003**, *278* (10), 8460−8467.
(67) Chang, E.; Donkin, S. S.; Teegarden, D. Parathyroid hormone suppresses insulin signaling in adipocytes. *Mol. Cell. Endocrinol.* **2009**, *307* (1), 77−82.
(68) Brunet, A.; Bonni, A.; Zigmond, M. J.; Lin, M. Z.; Juo, P.; Hu, L. S.; Anderson, M. J.; Arden, K. C.; Blenis, J.; Greenberg, M. E. Akt promotes cell survival by phosphorylating and inhibiting a Forkhead transcription factor. *Cell* **1999**, *96* (6), 857−868.
(69) Xie, X. W.; Liu, J. X.; Hu, B.; Xiao, W. Zebrafish foxo3b negatively regulates canonical Wnt signaling to affect early embryogenesis. *PLoS One* **2011**, *6* (9), e24469.
(70) Kagermeier-Schenk, B.; Wehner, D.; Özhan-Kizil, G.; Yamamoto, H.; Li, J.; Kirchner, K.; Hoffmann, C.; Stern, P.; Kikuchi, A.; Schambony, A.; Weidinger, G. Waif1/5T4 inhibits Wnt/β-catenin signaling and activates noncanonical Wnt pathways by modifying LRP6 subcellular localization. *Dev. Cell* **2011**, *21* (6), 1129−1143.
(71) Kaldis, P.; Pagano, M. Wnt signaling in mitosis. *Dev. Cell* **2009**, *17* (6), 749−750.
(72) Ridgeway, A. G.; Petropoulos, H.; Wilton, S.; Skerjanc, I. S. Wnt signaling regulates the function of MyoD and myogenin. *J. Biol. Chem.* **2000**, *275* (42), 32398−32405.
(73) Schambony, A.; Wedlich, D. Wnt signaling and cell migration. In *Madame Curie Bioscience Database [Internet]*. Landes Bioscience, Austin (TX); 2000−2013. https://www.ncbi.nlm.nih.gov/books/NBK6303/.
(74) Korzh, S.; Emelyanov, A.; Korzh, V. Developmental analysis of *ceruloplasmin* gene and liver formation in zebrafish. *Mech. Dev.* **2001**, *103* (1), 137−139.
(75) Sekine, K.; Chen, Y. R.; Kojima, N.; Ogata, K.; Fukamizu, A.; Miyajima, A. Foxo1 links insulin signaling to C/EBPα and regulates gluconeogenesis during liver development. *EMBO J.* **2007**, *26* (15), 3607−3615.
(76) Biemar, F.; Argenton, F.; Schmidtke, R.; Epperlein, S.; Peers, B.; Driever, W. Pancreas Development in Zebrafish: Early Dispersed Appearance of Endocrine Hormone Expressing Cells and Their Convergence to Form the Definitive Islet. *Dev. Biol.* **2001**, *230* (2), 189−203.
(77) Gerri, C.; Marín-Juez, R.; Marass, M.; Marks, A.; Maischein, H. M.; Stainier, D. Y. R. Hif-1α regulates macrophage-endothelial interactions during blood vessel development in zebrafish. *Nat. Commun.* **2017**, *8*, 15492.
(78) Lee, S.; Nakamura, E.; Yang, H.; Wei, W.; Linggi, M. S.; Sajan, M. P.; Farese, R. V.; Freeman, R. S.; Carter, B. D.; Kaelin, W. G.; Schlisio, S. Neuronal apoptosis linked to EglN3 prolyl hydroxylase and familial pheochromocytoma genes: developmental culling and cancer. *Cancer Cell* **2005**, *8* (2), 155−167.
(79) Bishop, T.; Gallagher, D.; Pascual, A.; Lygate, C. A.; de Bono, J. P.; Nicholls, L. G.; Ortega-Saenz, P.; Oster, H.; Wijeyekoon, B.; Sutherland, A. I.; Grosfeld, A.; Aragones, J.; Schneider, M.; van Geyte, K.; Teixeira, D.; Diez-Juan, A.; Lopez-Barneo, J.; Channon, K. M.; Maxwell, P. H.; Pugh, C. W.; Davies, A. M.; Carmeliet, P.; Ratcliffe, P. J. Abnormal sympathoadrenal development and systemic hypotension in PHD3−/− mice. *Mol. Cell. Biol.* **2008**, *28* (10), 3386−3400.
(80) Christine Hollander, M.; Poola-Kella, S.; Fornace, A. J., Jr Gadd34 functional domains involved in growth suppression and apoptosis. *Oncogene* **2003**, *22*, 3827.
(81) Quinlivan, V. H.; Farber, S. A. Lipid uptake, metabolism, and transport in the larval zebrafish. *Front. Endocrinol. (Lausanne, Switz.)* **2017**, *8*, 319.
(82) Yergeau, D. A.; Cornell, C. N.; Parker, S. K.; Zhou, Y.; Detrich, H. W. *bloodthirsty*, an RBCC/TRIM gene required for erythropoiesis in zebrafish. *Dev. Biol.* **2005**, *283* (1), 97−112.
(83) WHO. Dithiocarbamate pesticides, ethylenethiourea and propylenethiourea: a general introduction. In *International Program On Chemical Safety [Internet]*. 1998. http://www.inchem.org/documents/ehc/ehc/ehc78.htm.
(84) Haendel, M. A.; Tilton, F.; Bailey, G. S.; Tanguay, R. L. Developmental Toxicity of the Dithiocarbamate Pesticide Sodium Metam in Zebrafish. *Toxicol. Sci.* **2004**, *81* (2), 390−400.
(85) Tilton, F.; La Du, J. K.; Vue, M.; Alzarban, N.; Tanguay, R. L. Dithiocarbamates have a common toxic effect on zebrafish body axis formation. *Toxicol. Appl. Pharmacol.* **2006**, *216* (1), 55−68.

DOI: 10.1021/acs.est.8b04487
Environ. Sci. Technol. 2018, 52, 12829−12840

SUPPORTING INFORMATION

Down-Regulation of *hspb9* and *hspb11* Contributes to Wavy Notochord in Zebrafish Embryos Following Exposure to Polychlorinated Diphenylsulfides

Rui Zhang,[†] Xiaoxiang Wang,[‡,§] Xuesheng Zhang,[⊥] Junjiang Zhang,[‡] Xiaowei Zhang,[‡] Xiao Shi,[∥] Doug Crump,[¶] Robert J. Letcher,[¶] John P. Giesy,[▽] and Chunsheng Liu[*,○]

[†]School of Resources and Environment, University of Jinan, Jinan 250022, P. R. China.

[○]College of Fisheries, Huazhong Agricultural University, Wuhan 430070, P. R. China.

[‡]State Key Laboratory of Pollution Control and Resources Reuse, School of the Environment, Nanjing University, Nanjing 210023, P. R. China.

[§]Association of Chinese Chemists and Chemical Engineers in Germany, Limburgerhof 67117, Germany.

[⊥]School of Resources and Environmental Engineering, Anhui University, Hefei 230601, P. R. China.

[∥]Center for Reproductive Medicine, Department of Obstetrics and Gynaecology, Nanfang Hospital, Southern Medical University, Guangzhou 510515, P. R. China.

[¶]Ecotoxicology and Wildlife Health Division, Environment and Climate Change Canada, National Wildlife Research Centre, Carleton University, 1125 Colonel By Drive, Ottawa, K1A 0H3, Canada.

[▽]Department of Veterinary Biomedical Sciences and Toxicology Centre, University of Saskatchewan, Saskatoon, Saskatoon, SK S7N 5B3, Canada.

[*]**Author for correspondence:**

College of Fisheries, Huazhong Agricultural University, Wuhan 430070, China

Tel: 86 27 87282113, Fax: 86 27 87282114, E-mail: cliu@mail.hzau.edu.cn

Number of pages: 19; Number of figures: 7; Number of tables: 8

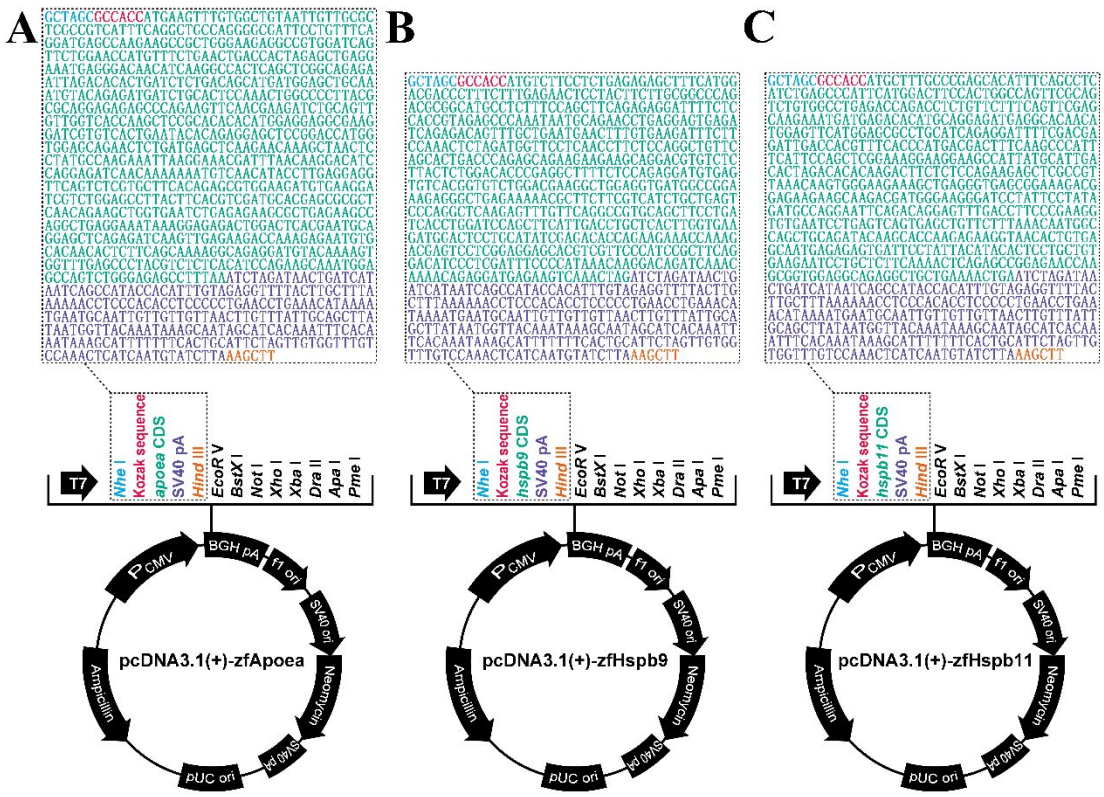

Figure S1. Detailed plasmid maps and sequences of pcDNA3.1(+)-zfApoea (A), pcDNA3.1(+)-zfHspb9 (B) and pcDNA3.1(+)-zfHspb11 (C).

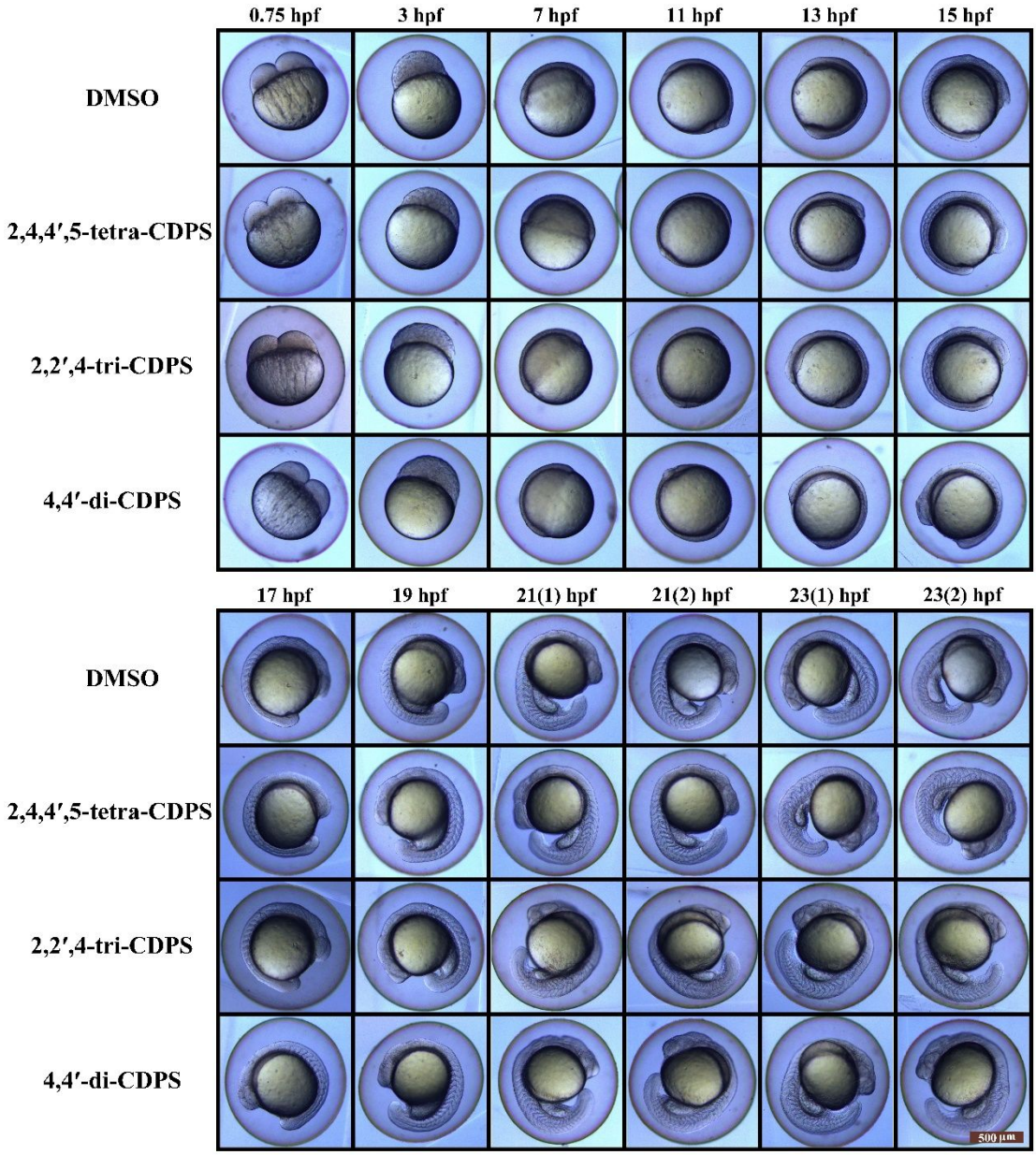

Figure S2. Time-course morphological analysis to capture time of onset of notochord kinks and twists induced by exposure to 2500 nM of 2,4,4′,5-tetra-CDPS, 2,2′,4-tri-CDPS or 4,4′-di-CDPS. Two representative images of developing embryos at 21 and 23 hpf were shown. Scale bar: 500 μm in 70.8× magnification.

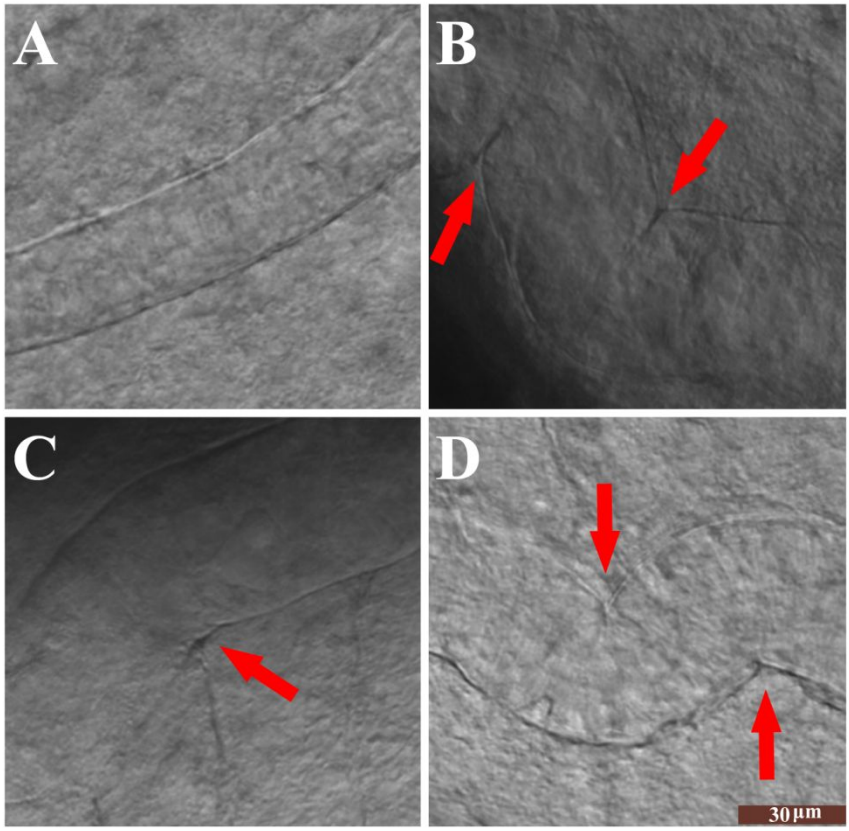

Figure S3. Representative confocal micrographs of notochord of zebrafish embryos exposed to 0.5% (v/v) DMSO (A), 2500 mM 2,4,4′,5-tetra-CDPS (B), 2,2′,4-tri-CDPS (C) or 4,4′-di-CDPS (D) at 21 hpf. The arrows indicate kinks caused by PCDPS exposure. Scale bar: 30 µm in 103 × magnification.

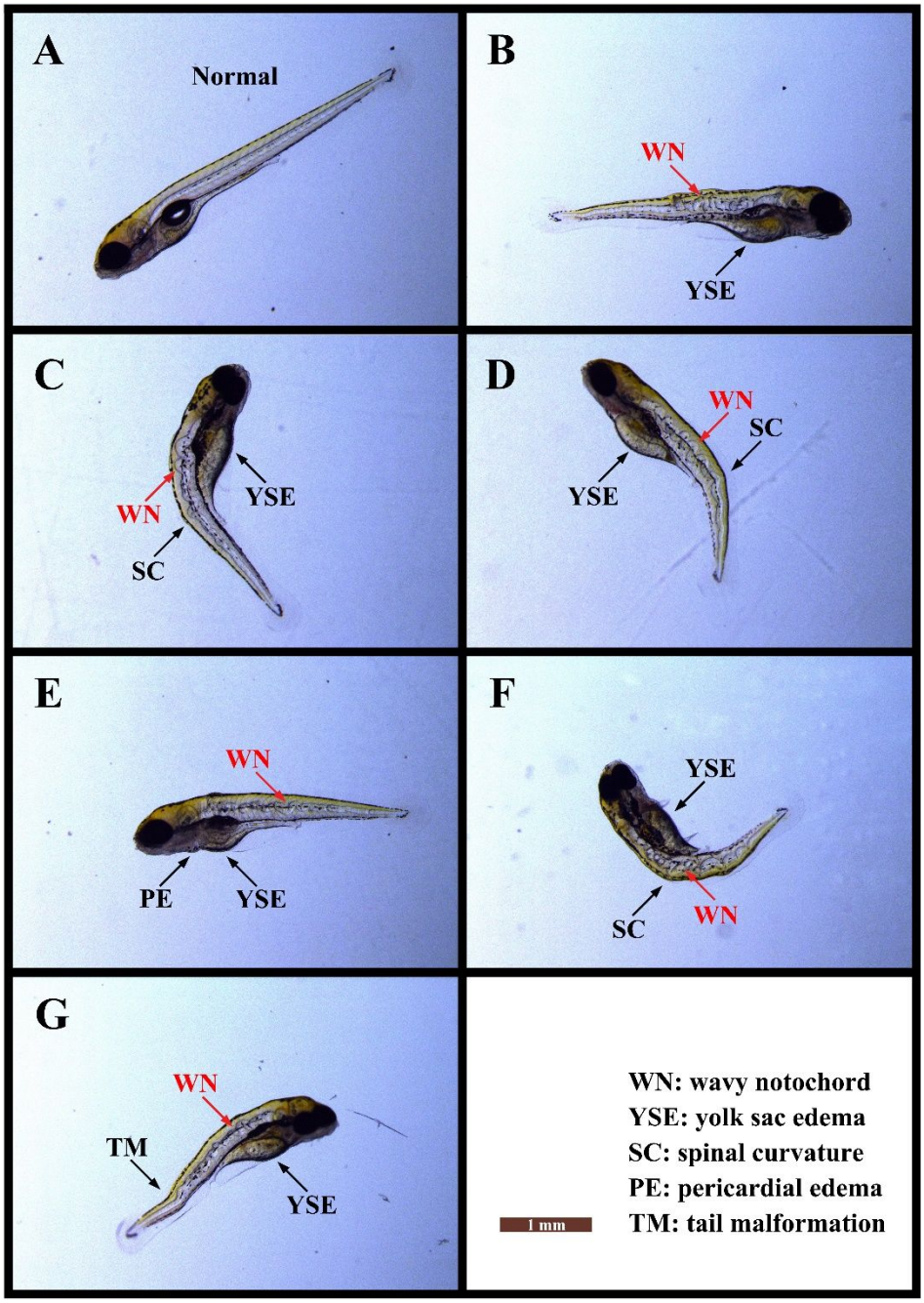

Figure S4. Representative optical images of deformed zebrafish larvae following exposure to 0.5% DMSO (A), 2500 nM 2,2',3,3',4,5,6-hepta-CDPS (B), 500 nM 2,3,3',4,5,6-hexa-CDPS (C), 2500 nM 2,2',3',4,5-penta-CDPS (D), 2500 nM 2,4,4′,5-tetra-CDPS (E), 2500 nM 2,2′,4-tri-CDPS (F) or 2500 nM 4,4′-di-CDPS (G) at 120 hpf. Types of malformation observed included yolk sac edema (YSE), spinal

curvature (SC), pericardial edema (PE), tail malformation (TM), and a unique wavy notochord (WN) that was not observed in dioxin-exposed zebrafish. Scale bar: 1 mm in 27.7× magnification.

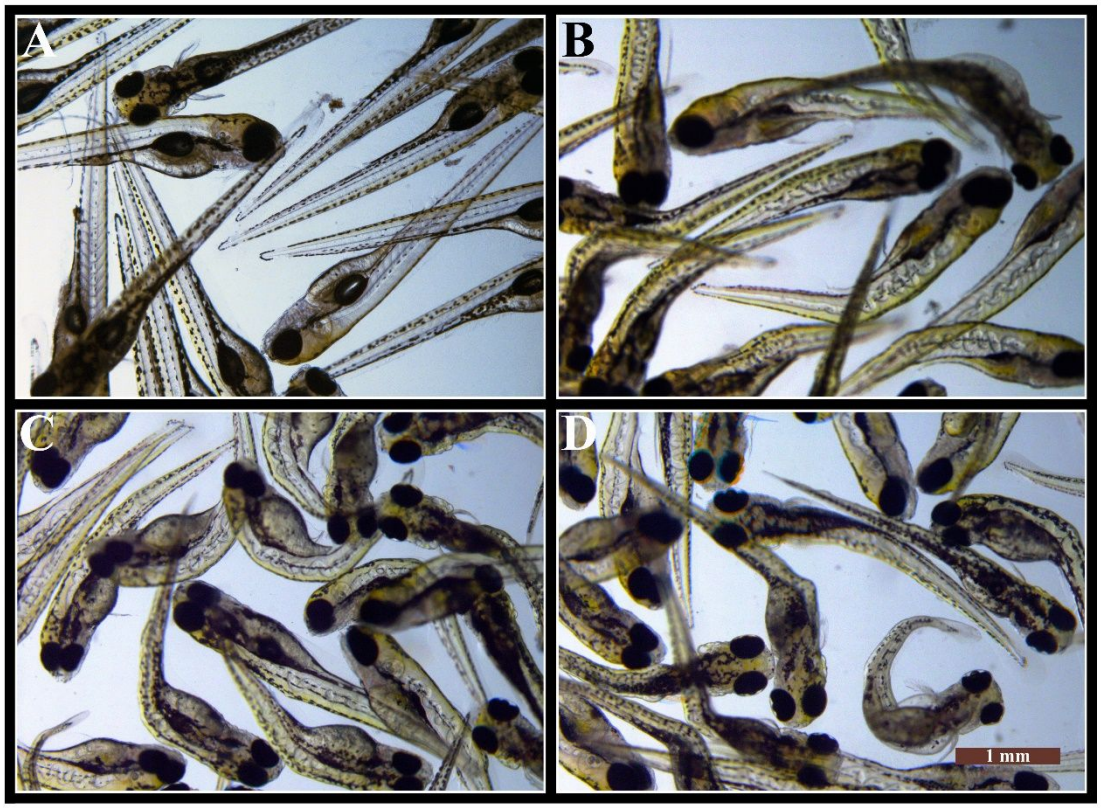

Figure S5. Wavy notochords were present in almost all of the deformed zebrafish larvae following exposure to 2500 nM of 2,4,4′,5-tetra-CDPS (B), 2,2′,4-tri-CDPS (C) or 4,4′-di-CDPS (D) at 120 hpf. Normal notochords of DMSO-exposed zebrafish larvae are shown in panel A. Scale bar: 1 mm in 27.5× magnification.

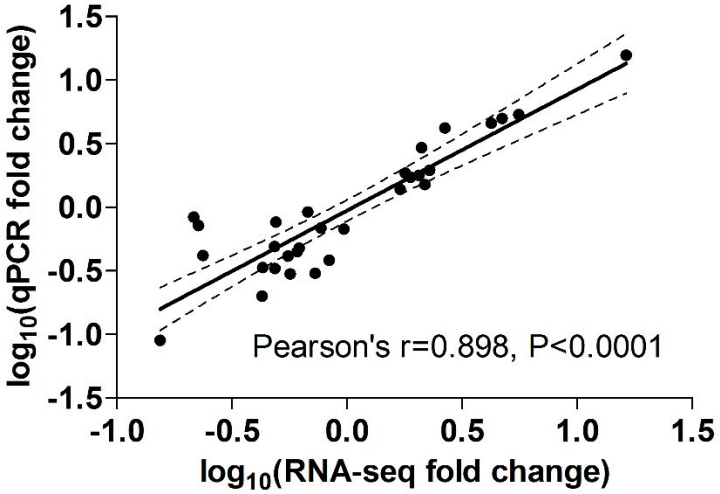

Figure S6. Linear regression analysis comparing $\log_{10}$-transformed fold-change values derived from qRT-PCR with those obtained from RNA-seq. Points represent the fold change in mRNA expression of genes selected from each treatment group. The dotted lines represent 95% confidence intervals.

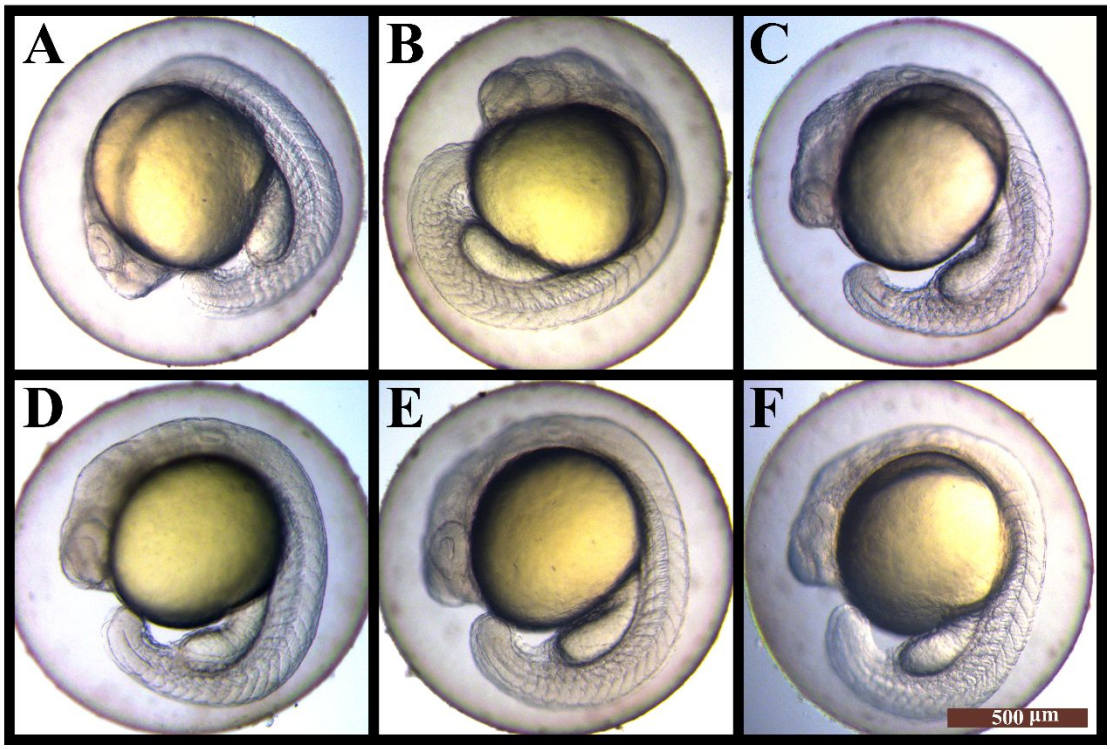

Figure S7. Representative images of rescued notochord phenotypes in *hspb9* or *hspb11* mRNA-injected embryos following exposure to 4,4′-di-CDPS (A for *hspb9*, D for *hspb11*), 2,2′,4-tri-CDPS (B for *hspb9*, E for *hspb11*) or 2,4,4′,5-tetra-CDPS (C for *hspb9*, F for *hspb11*) at 21 hpf.

Table S1. Retention time and quantitative ions of PCDPS congeners tested and the internal standard.

Compound	RT (min)	Quantitative ions (m/z)
^{13}C-PCB-31	11.15	268, 198
2,4,4′,5-tetra-CDPS	16.10	324, 254
2,2′,4-tri-CDPS	15.12	288, 220, 218
4,4′-di-CDPS	12.14	254, 218, 184

Table S2. Recoveries of individual PCDPS congeners in exposure solutions and zebrafish embryos (n=3; data represent mean ± SD).

Compound	Exposure solution (%)	Zebrafish embryos (%)
2,4,4′,5-tetra-CDPS	110.6±10.4	105.5±9.7
2,2′,4-tri-CDPS	89.8±8.1	68.5±8.2
4,4′-di-CDPS	88.3±7.9	63.7±7.6

Table S3. Primer sequences of the selected differentially expressed genes and reference gene (*rpl8*) in zebrafish for qRT-PCR.

Gene	Forward Sequence (5'-3')	Reverse Sequence (5'-3')	Accession number
apoea	gacacactgatctctgacagca	atcttcgttgaacttctgggct	NM_001020565.1
btr30	agcaggcttcatttaatctctggac	tgagtgcgatctgggcaaac	NM_200422.1
cyp1a	gcattacgatacgttcgataaggac	gctccgaataggtcattgacgat	NM_131879.2
egln3	gcattcgtgcgaggtcaaaggc	gcaatcccccatgttccttggca	NM_213310.1
hspb9	tggacgacccttttctttgag	gcattatttgggctctacgg	NM_001114705.2
hspb11	gagatgaggcacaacatgga	ttgtttaacggcgagctctt	NM_001099427.1
mt2	ctgcgaatgtgccaagactg	aacgcagacgtggagtagac	NM_001131053.2
ppp1r15a	gaagagcagtgggaagaagg	ctgaactctcctcctgaaacg	NM_001082921.1
slc27a2a	ttagagtctggtgcgtcctg	acggttctgctgcttatga	NM_001025299.1
sult6b1	gtgggcgactggaagaatca	ctgcactggtgaaatcctgt	NM_214686.1
rpl8	ttgttggtgttgttgctggt	ggatgctcaacaggggttcat	NM_200713

Table S4. Sequences of siRNA oligo-duplexes employed to knock down mRNA expression of specific endogenous genes in zebrafish embryos.

Target Gene	Sense (5'-3')	Anti-sense (5'-3')	Accession number
hspb9	gaaugaacuuugugaagauuu	aucuucacaaaguucauucuu	NM_001114705.2
hspb11	gagcaaugagagagugauuuu	aaucacucucucauugcucuu	NM_001099427.1
negative control	uucuccgaacgugucacgutt	acgugacacguucggagaatt	——

Table S5. Measured concentrations in exposure solutions (nM) and zebrafish larvae (μg/g wet mass (wm)) following exposure to 2500 nM of three individual PCDPS congeners, and the corresponding bioconcentration factors (BCFs) at 21 hpf. Measured concentrations represent the mean of three replicates ± SE. BCF value was calculated as the ratio of measured concentration in zebrafish embryos (μg/g, wm) to that in exposure medium (μg/mL) at 21 hpf.

Compound	Nominal concentration (nM)	Measured concentration		BCF
		Exposure solution (nM)	Zebrafish embryos (μg/g ww)	
2,4,4′,5-tetra-CDPS	2500	2439±24.1	236±7.0	299
2,2′,4-tri-CDPS		2447±35.4	174±8.8	333
4,4′-di-CDPS		2410±25.9	197±12	384

Table S6. List of differentially expressed genes (DEGs) in zebrafish embryos exposed to 2500 nM of 2,4,4′,5-tetra-CDPS, 2,2′,4-tri-CDPS or 4,4′-di-CDPS, compared with DMSO-treated control at 21 hpf. Genes with a false discovery rate (FDR) *q* value < 0.05 were identified as DEGs using DESeq R package.

Gene	Gene full name/gene description	Ensembl ID	NCBI accession #	Fold change (FDR *q* value)		
				2,4,4′,5-tetra-CDPS	2,2′,4-tri-CDPS	4,4′-di-CDPS
rd37	*ankyrin repeat domain 37*	ENSDARG00000056376	NM_001145614	0.773 (1)[†]	0.269 (3.71×10^{-4})	0.392 (0.142)[†]
a4b.2	*apolipoprotein a-IV b, tandem duplicate 2*	ENSDARG00000020866	NM_001128758	1.61 (1.16×10^{-3})	1.32 (0.0808)[†]	1.37 (0.198)[†]
ea	*apolipoprotein ea*	ENSDARG00000102004	NM_001020565	2.06 (2.09×10^{-5})	1.79 (5.12×10^{-5})	2.18 (7.01×10^{-8})
t	*betaine-homocysteine methyltransferase*	ENSDARG00000013430	NM_001012480	0.939 (1)[†]	0.707 (3.73×10^{-3})	0.751 (0.176)[†]
0	*bloodthirsty-related gene family, member 30*	ENSDARG00000104912	NM_200422	0.227 (1.23×10^{-3})	0.771 (1)[†]	0.216 (1.89×10^{-4})
23060.3	*a long intergenic non-coding RNA*[‡]	ENSDARG00000105651	NA	0.726 (1)[†]	0.286 (0.0455)	0.441 (1)[†]
71955.3	*bx571955.3*[‡]	ENSDARG00000099324	NA	0.589 (1)[†]	0.032 (9.17×10^{-6})	0.504 (1)[†]
z01103941.1	*cabz01103941.1*[‡]	ENSDARG00000105129	NA	0.871 (1)[†]	0.714 (0.0166)	0.730 (0.0651)[†]
n1	*claudin 1*	ENSDARG00000040045	NM_131770	0.709 (0.208)[†]	0.728 (0.0162)	0.798 (0.673)[†]
o1a	*coronin, actin binding protein, 1a*	ENSDARG00000054610	NM_201114	0.422 (0.0908)[†]	0.459 (0.0413)	0.465 (0.312)[†]
x	*coproporphyrinogen oxidase*	ENSDARG00000062025	NM_001040094	0.885 (1)[†]	0.717 (0.0351)	0.789 (0.885)[†]
88008.1	*cr388008.1*[‡]	ENSDARG00000104748	NA	1.79 (1)[†]	3.44 (0.0295)	3.12 (0.166)[†]
30712.1	*ct030712.1*[‡]	ENSDARG00000044355	NA	0.488 (6.17×10^{-3})	0.696 (0.981)[†]	0.462 (0.491)[†]
41402.1	*cu041402.1*[‡]	ENSDARG00000098072	NA	1.018 (1)[†]	0.0250 (0.0332)	0.023 (0.0651)[†]
1a	*cytochrome p450, family 1, subfamily a*	ENSDARG00000098315	NM_131879	16.3 (1.82×10^{-39})	5.58 (2.15×10^{-16})	4.73 (5.48×10^{-9})
1b1	*cytochrome p450, family 1, subfamily b, polypeptide 1*	ENSDARG00000068934	NM_001045256	4.10 (3.33×10^{-3})	2.12 (0.282)[†]	2.12 (0.491)[†]
24a1	*cytochrome p450, family 24, subfamily a, polypeptide 1*	ENSDARG00000103277	NM_001089458	0.752 (1)[†]	0.491 (0.246)[†]	0.388 (3.79×10^{-4})
a3	*egl-9 family hypoxia-inducible factor 3*	ENSDARG00000032553	NM_213310	0.836 (1)[†]	0.154 (3.51×10^{-5})	0.237 (8.30×10^{-3})
m1	*filamin binding lim protein 1*	ENSDARG00000071558	NM_001077303	0.711 (1)[†]	0.611 (0.0413)	0.652 (0.417)[†]

o3b	*forkhead box o3b*	ENSDARG00000042904	NM_131085	1.16 (1)[†]	1.49 (0.0413)	1.16 (1)[†]
at	*guanidinoacetate n-methyltransferase*	ENSDARG00000070844	NM_001105595	1.01 (1)[†]	0.689 (0.0413)	0.766 (1)[†]
m	*glycine amidinotransferase (l-arginine:glycine amidinotransferase)*	ENSDARG00000036239	NM_199531	1.06 (1)[†]	0.754 (0.0413)	0.824 (0.909)[†]
l2ipb	*glutamate receptor, ionotropic, delta 2 (grid2) interacting protein, b*	ENSDARG00000095603	NM_001044903	0.762 (1)[†]	0.596 (0.0351)	0.719 (1)[†]
b11	*heat shock protein beta-11*	ENSDARG00000002204	NM_001099427	0.555 (1.12×10^{-3})	0.607 (5.41×10^{-5})	0.567 (1.96×10^{-5})
b9	*heat shock protein, alpha-crystallin-related, 9*	ENSDARG00000078674	NM_001114705	0.431 (9.75×10^{-7})	0.491 (1.01×10^{-5})	0.487 (5.89×10^{-6})
p1a	*insulin-like growth factor binding protein 1a*	ENSDARG00000099351	NM_173283	0.832 (1)[†]	0.494 (7.38×10^{-3})	0.620 (0.491)[†]
g1	*insulin induced gene 1*	ENSDARG00000010658	NM_199869	0.879 (1)[†]	0.666 (0.0413)	0.698 (0.312)[†]
a	*insulin receptor substrate 2a*	ENSDARG00000037099	NM_200315	0.807 (1)[†]	0.492 (9.58×10^{-3})	0.542 (0.130)[†]
p1	*lysosomal associated membrane protein 1*	ENSDARG00000100181	NA	0.742 (1)[†]	0.621 (5.63×10^{-3})	0.675 (0.261)[†]
1	*lymphocyte cytosolic protein 1 (L-plastin)*	ENSDARG00000023188	NM_131320	0.693 (1)[†]	0.603 (0.0413)	0.616 (0.218)[†]
101882355	*transmembrane protein 43-like*[‡]	ENSDARG00000098297	NA	0.792 (1)[†]	0.670 (0.0183)	0.736 (0.520)[†]
568866	*serine/threonine-protein kinase pim-1-like*[‡]	ENSDARG00000093733	NA	0.909 (1)[†]	0.361 (0.0759)[†]	0.257 (0.0460)
	metallothionein 2	ENSDARG00000041623	NM_001131053	4.23 (2.96×10^{-13})	2.11 (2.67×10^{-7})	2.67 (1.94×10^{-10})
a1b	*prolyl 4-hydroxylase, alpha polypeptide I b*	ENSDARG00000071082	NM_214691	0.952 (1)[†]	0.564 (0.0351)	0.716 (1)[†]
b3	*6-phosphofructo-2-kinase/fructose-2,6-biphosphatase 3*	ENSDARG00000001953	NM_213397	0.821 (1)[†]	0.508 (0.0146)	0.549 (0.142)[†]
2	*pim-2 proto-oncogene, serine/threonine kinase*	ENSDARG00000059001	NM_131539	0.947 (1)[†]	0.634 (0.0378)	0.666 (0.312)[†]
-	*pyruvate kinase L/R*	ENSDARG00000042010	NM_201289	1.05 (1)[†]	0.699 (0.0413)	0.783 (1)[†]
5b	*purine nucleoside phosphorylase 5b*	ENSDARG00000099802	NM_001004628	0.812 (1)[†]	0.419 (7.00×10^{-5})	0.662 (0.830)[†]
1r15a	*protein phosphatase 1, regulatory subunit 15a*	ENSDARG00000069135	NM_001082921	0.728 (1)[†]	0.428 (2.01×10^{-4})	0.484 (0.0111)
1r3da	*protein phosphatase 1, regulatory subunit 3da*	ENSDARG00000077513	NM_001110412	0.549 (1)[†]	0.347 (5.63×10^{-3})	0.412 (0.105)[†]
x1	*peroxiredoxin 1*	ENSDARG00000058734	NM_001013471	1.57 (0.207)[†]	1.60 (0.0345)	1.50 (0.319)[†]
1b	*parathyroid hormone 1b*	ENSDARG00000091961	NM_212949	0.220 (0.617)[†]	0.081 (2.97×10^{-3})	0.173 (0.160)[†]

d1	*ras, dexamethasone-induced 1*	ENSDARG00000019274	NM_200532	1.06 (1)[†]	0.606 (4.51×10^{-3})	0.629 (0.0674)[†]
5	*RNA binding motif protein 5*	ENSDARG00000098280	NM_001100138	0.803 (1)[†]	0.718 (0.0260)	0.756 (0.319)[†]
h211-117m20.	*transcobalamin-like*[‡]	ENSDARG00000091996	NM_001252649	2.87 (0.294)[†]	4.00 (5.12×10^{-5})	2.60 (0.261)[†]
h211-195b15.8	*dual specificity protein phosphatase 16-like*[‡]	ENSDARG00000094836	NA	0.857 (1)[†]	0.617 (0.0413)	0.662 (0.491)[†]
h211-211k8.12	*si:ch211-211k8.12*[‡]	ENSDARG00000104986	NA	0.520 (1)[†]	0.280 (3.86×10^{-4})	0.477 (0.614)[†]
key-66g10.2	*cytokine activity*[‡]	ENSDARG00000092845	NA	0.795 (1)[†]	0.298 (0.0413)	0.465 (0.999)[†]
key-85k7.7	*si:dkey-85k7.7*[‡]	ENSDARG00000101135	NA	0.860 (1)[†]	0.259 (0.0184)	0.382 (0.614)[†]
7a2a	*solute carrier family 27 (fatty acid transporter), member 2a*	ENSDARG00000036237	NM_001025299	0.971 (1)[†]	0.620 (3.51×10^{-5})	0.676 (0.0418)
6b1	*sulfotransferase family, cytosolic, 6b, member 1*	ENSDARG00000086826	NM_214686	2.28 (9.69×10^{-15})	1.90 (6.29×10^{-14})	1.71 (1.38×10^{-4})
gl	*trophoblast glycoprotein-like*	ENSDARG00000099609	NM_194392	1.04 (1)[†]	1.46 (7.34×10^{-3})	1.34 (1)[†]
1	*WD repeat and SOCS box containing 1*	ENSDARG00000021343	NM_199633	0.867 (1)[†]	0.604 (0.0413)	0.688 (0.747)[†]
fb18f06	*wu:fb18f06*[‡]	ENSDARG00000097635	NA	1.20 (1)[†]	6.79 (2.23×10^{-3})	0.886 (1)[†]
fc75a09	*wu:fc75a09*[‡]	ENSDARG00000089342	NA	1.36 (1)[†]	1.65 (0.0140)	1.32 (1)[†]
:171927	*zgc:171927*[‡]	ENSDARG00000033056	NM_001102642	16.0 (1)[†]	45.8 (0.0295)	18.0 (1)[†]
:172090	*zgc:172090*[‡]	ENSDARG00000075626	NM_001128253	0.440 (0.976)[†]	0.262 (0.0102)	0.459 (0.775)[†]
1069	*zinc finger protein 1069*	ENSDARG00000104124	NM_001109867	0.932 (1)[†]	1.96 (0.540)[†]	2.67 (3.32×10^{-3})

[†]Not identified as DEGs because the FDR *q* value is greater or equal to 0.05.

[‡]Uncharacterized gene.

NA: Not available.

Table S7. Comparison of relative fold changes in expression of mRNA determined by use of RNA-seq and qRT-PCR.

Gene	2,4,4′,5-tetra-CDPS		2,2′,4-tri-CDPS		4,4′-di-CDPS	
	RNA-seq	qRT-PCR	RNA-seq	qRT-PCR	RNA-seq	qRT-PCR
apoea	2.05	1.79	1.79	1.86	2.18	1.51
btr30	0.227	0.719	0.771	0.686	0.216	0.841
cyp1a	16.34	15.75	5.58	5.37	4.73	5.00
egln3	0.836	0.384	0.154	0.090	0.237	0.417
hspb11	0.555	0.412	0.607	0.447	0.567	0.299
hspb9	0.431	0.336	0.491	0.767	0.487	0.331
mt2	4.23	4.59	2.11	2.94	2.67	4.21
ppp1r15a	0.728	0.303	0.428	0.200	0.484	0.492
slc27a2a	0.971	0.675	0.620	0.478	0.676	0.921
sult6b1	2.28	1.96	1.90	1.73	1.70	1.38

Table S8. The fold change of target mRNA expression (determined by qRT-PCR) in zebrafish embryos injected with *hspb9* and *hspb11* siRNA or *apoea* mRNA at 21 hpf. Data represent the average of three technical replicates ± SE.

Zebrafish embryos injected with siRNA or mRNA	**Fold change±SE**
100 pg of *hspb9* siRNA	0.863±0.07
400 pg of *hspb11* siRNA	0.579±0.16
400 pg of *apoea* mRNA	17.5±0.9